

**Journal:** Physical Review E

**Accession code:** EU12660

**Article Title:** Conditioning the complexity of random landscapes on marginal optima

**First Author:** Jaron Kent-Dobias

#### AUTHOR QUERIES - TO BE ANSWERED BY THE CORRESPONDING AUTHOR

The following queries have arisen during the typesetting of your manuscript. Please answer these queries by marking the required corrections at the appropriate point in the text.

1	Please see <a href="https://journals.aps.org/authors/logarithms-h14">https://journals.aps.org/authors/logarithms-h14</a> for Physical Review guidelines on logarithmic notation.
2	Please verify light face ' $\omega$ ' throughout.
3	Please verify definition of "BRST."
4	Please see <a href="http://publish.aps.org/authors/multiplication-signs-h11">http://publish.aps.org/authors/multiplication-signs-h11</a> for information on the use of multiplication signs.
5	Please see <a href="https://journals.aps.org/authors/new-novel-policy-physical-review">https://journals.aps.org/authors/new-novel-policy-physical-review</a> for Physical Review policy on use of "new" and priority claims.
6	Please verify definition of "TAP."
7	Please ensure that all book references contain publisher city.
8	Please update eprints with published journal reference if possible/appropriate.
9	The citation of Ref. [23] is missing in the text. Please cite the same in running text in sequence to avoid the renumbering of references.
FQ	This funding provider could not be uniquely identified during our search of the FundRef registry (or no Contract or Grant number was detected). Please check information and amend if incomplete or incorrect.
Q	This reference could not be uniquely identified due to incomplete information or improper format. Please check all information and amend if applicable.

## Important Notice to Authors

Attached is a PDF proof of your forthcoming article in PRE. Your article has 21 pages and the Accession Code is **EU12660**.

Your paper will be in the following section of the journal: REGULAR ARTICLES

No further publication processing will occur until we receive your response to this proof.

All articles, regardless of their original source, are converted into standardized XML, which is then used to create the PDF and online versions of the article as well as to populate third-party systems such as Portico, Crossref, and Web of Science. This process works exceptionally well for most articles; however, please check carefully all key elements of your PDF proof, particularly any equations or tables.

### ORCID <https://orcid.org/>

- Follow any ORCID links (🔗) after the authors' names and verify that they point to the appropriate record.
- Requests to add ORCIDs should be sent only during the first proof revisions (not before or after). If authors do not subsequently add/authenticate ORCIDs within seven business days, production of the paper will proceed and no further requests to add ORCIDs will be processed. See complete details regarding ORCID requests and ORCID verification at <https://journals.aps.org/authors/addingorcids-during-proof-corrections>.
- If this paper is an Erratum or a Reply, the corresponding author's ORCID may be present if previously provided to APS, but no ORCIDs can be added at proof stage.

### Research Organization Registry ID (ROR) <https://ror.org/>

- Ensure affiliations have been correctly identified by clicking on any institution names that have been linked to the ROR database (blue text). Note that affiliations will be linked to their parent institution's ROR ID (if available) if they do not have a separate ID. If no appropriate ID is available, there will be no link. Links cannot be removed for correctly linked affiliations.
- Information about an author's research organization is submitted to Crossref as part of the metadata for articles published by APS.

### Crossref Funder Registry ID <https://www.crossref.org/services/funder-registry/>

- Ensure acknowledgments include all sources of funding for your article, following any requirements of your funding sources. Where possible, please include grant and award ids.
- Information about an article's funding sources is submitted to Crossref to help you comply with funding agency mandates. Crossref's Funder Registry is the definitive registry of funding agencies.

Please carefully check the following funder information we have already extracted from your article and ensure its accuracy and completeness:

- INFN

Overall, please proofread the entire formatted article very carefully. The redlined PDF should be used as a guide to see changes that were made during copyediting. However, note that some changes to math and/or layout may not be indicated.

### Other Items to Check

- All key elements of the paper, particularly the equations and tabular data. (The original manuscript has been converted to XML prior to the creation of the PDF proof, as described above.)
- Title: It may have changed during the peer-review process.
- Author list: Ensure all names are spelled correctly and all authors are presented in the appropriate order, especially if you have used grouped addresses in REVTeX, which will order authors by institution, not in the order they were entered.
- Contact author: Ensure there is a byline footnote containing the email address for each contact author if desired (Contact author: [author@email.com](mailto:author@email.com)). All emails will be labeled as contact authors to ensure they are picked up by indexing services. A contact author on the published paper does not have to be the corresponding author (see <https://journals.aps.org/authors/editorial-policies-authorship#responsibilities>).
- Affiliations: Affiliation(s) must be where the research was conducted. Ensure institution names are spelled correctly and attributed to the appropriate author(s). Click on any institution names that have been linked to the ROR database (blue text) to ensure they are correctly identified.
- Receipt date: Please confirm accuracy.

- Acknowledgments: Appropriately acknowledge all funding sources.
- Hyphenation: Please note APS style:
  - Hyphens may have been inserted in word pairs that function as adjectives when they occur before a noun, as in “gamma-ray detection,” “4-mm-long gas cell,” and “R-matrix theory.”
  - Hyphens are deleted from word pairs when they are not used as adjectives before nouns, as in “electric fields of gamma rays,” “was 4 mm in length,” and “the R matrix is tested.”
  - Hyphens are not used after prefixes or before suffixes: superresolution, quasiequilibrium, nanoprecipitates, resonancelike, clockwise.
- Figures:
  - Ensure they are accurate and sized properly.
  - Check that all labeling is legible.
  - If you revise any figures, please indicate clearly if any data or results have changed.
  - Figure quality in the proof is representative of the quality to be used in the online journal. Some compression and downsampling of figures may have occurred. Fine details may have become somewhat fuzzy, especially in color figures. The print journal uses higher resolution files and therefore details may be sharper in print.
  - Figures submitted as separate files containing color appear in color on these proofs and in the online journal.
  - For information on color in the print journal see <https://journals.aps.org/prl/authors#pubcharges>.
- References: Ensure article titles are provided, as appropriate for the journal.
- Supplemental material (SM): Files will not be copyedited or altered by APS after submission and should be submitted in a format ready to be published. You will not receive page proofs of SM. All references cited in SM should be listed in the reference section of the main text. For more information see <https://journals.aps.org/authors/supplemental-material-instructions>.

## Ways to Respond

- Web: If you accessed this proof online, follow the instructions on the web page to submit corrections.
- Email: Send corrections to [preproofs@aptaracorp.com](mailto:preproofs@aptaracorp.com)

# Conditioning the complexity of random landscapes on marginal optima

Jaron Kent-Dobias \*

*Istituto Nazionale di Fisica Nucleare, Sezione di Roma I, Rome 00184, Italy*



(Received 24 July 2024; accepted 2 December 2024; published xxxxxxxxx)

Marginal optima are minima or maxima of a function with many nearly flat directions. In settings with many competing optima, marginal ones tend to attract algorithms and physical dynamics. Often, the important family of marginal attractors is a vanishing minority compared with nonmarginal optima and other unstable stationary points. We introduce a generic technique for conditioning the statistics of stationary points in random landscapes on their marginality and apply it in three isotropic settings with qualitatively different structures: in the spherical spin-glasses, where the energy is Gaussian and its Hessian is a Gaussian orthogonal ensemble (GOE); in multispherical spin glasses, which are Gaussian but non-GOE; and in sums of squared spherical random functions, which are non-Gaussian. In these problems, we are able to fully characterize the distribution of marginal optima in the landscape, including when they are in the minority.

DOI: [10.1103/PhysRevE.00.004100](https://doi.org/10.1103/PhysRevE.00.004100)

## I. INTRODUCTION

Systems with rugged landscapes are important across many disciplines, from the physics of glasses and spin glasses to statistical inference problems [1]. The behavior of these systems is best understood when equilibrium or optimal solutions are studied and weighted averages can be taken statically over all possible configurations. However, such systems are also infamous for their tendency to defy equilibrium and optimal expectations in practice due to the presence of dynamic transitions or crossovers that leave physical or algorithmic dynamics stuck exploring only a subset of configurations [2,3].

In mean-field settings, it was long thought that physical and many algorithmic dynamics would get stuck at a specific energy level, called the threshold energy. The threshold energy is the energy level at which level sets of the landscape transition from containing mostly saddle points to containing mostly minima. The level set associated with this threshold energy contains mostly *marginal minima*, or minima whose Hessian matrix have a continuous spectral density over all sufficiently small positive eigenvalues. In most circumstances the spectrum is *pseudogapped*, which means that the spectral density smoothly approaches zero as zero eigenvalue is approached from above.

However, recent work found that the threshold energy is not important even for simple gradient descent dynamics [4–6]. Depending on the initial condition of the system and the nature of the dynamics, the energy reached can be above or below the threshold energy, while in some models the threshold energy is completely inaccessible to any dynamics [7]. Though it is still not known how to predict the energy level that many simple algorithms will reach, the results all share one commonality: the minima found are still marginal despite being in the minority compared to stiff minima or saddle

points. This ubiquity of behavior suggests that the distribution of marginal minima can be used to bound out-of-equilibrium dynamical behavior.

Despite their importance in a wide variety of in- and out-of-equilibrium settings [8–17], it is not straightforward to condition on the marginality of minima using the traditional methods for analyzing the distribution of minima in rugged landscapes. Using the method of a Legendre transformation of the Parisi parameter corresponding to a set of real replicas, one can force the result to correspond with marginal minima by tuning the value of that parameter [18]. However, this results only in a characterization of the threshold energy and cannot characterize marginal minima at other energies where they are a minority.

The alternative approach, used to great success in the spherical spin glasses, is to start by understanding in detail the Hessian matrix at stationary points. Then, one can condition the analysis on whatever properties of the Hessian are necessary to lead to marginal minima. This strategy is successful in spherical spin glasses because it is straightforward to implement. First, the shape of the Hessian's spectrum is independent of energy, regardless of whether one sits at a stationary point. This is a property of models whose energy is a Gaussian random variable [19,20]. Furthermore, a natural parameter in the analysis of these models linearly shifts the spectrum of the Hessian. Therefore, tuning this parameter to a specific constant value allows one to require that the Hessian spectrum has a pseudogap and therefore that the associated minima be marginal. Unfortunately, this strategy is less straightforward to generalize to other models. Many models of interest, especially in inference problems, have Hessian statistics that are poorly understood. This is especially true for the statistics of the Hessian conditioned to lie at stationary points, which is necessary to understand in models whose energy is non-Gaussian.

Here, we introduce a generic method for conditioning the statistics of stationary points on their marginality. The tech-

\*Contact author: [jaron.kent-dobias@roma1.infn.it](mailto:jaron.kent-dobias@roma1.infn.it)

nique makes use of a novel way to condition an integration measure to select only configurations that result in a certain value of the smallest eigenvalue of a matrix. By requiring that the smallest eigenvalue of the Hessian at stationary points be zero and further looking for a sign that the zero eigenvalue lies at the edge of a continuous spectrum, we enforce the condition that the spectrum has a pseudogap and is therefore marginal. We demonstrate the method on the spherical spin glasses, where it is unnecessary but instructive, and on extensions of the spherical models where the technique is more useful. In related work, we compare the marginal complexity with the performance of gradient descent and approximate message-passing algorithms [21].

An outline of this paper follows. In Sec. II we introduce the technique for conditioning on the smallest eigenvalue and how to extend it to further condition on the presence of a pseudogap. We provide a simple but illustrative example using a Gaussian orthogonal ensemble (GOE) matrix with a shifted diagonal. In Sec. III we apply this technique to the problem of characterizing marginal minima in random landscapes. Section IV gives several examples of the marginal complexity applied to specific models of increasing difficulty. Finally, Sec. V summarizes this work and suggests necessary extensions.

## II. CONDITIONING ON THE SMALLEST EIGENVALUE

In this section, we introduce a general method for conditioning a measure on the smallest eigenvalue of some matrix that depends on it. In Sec. II B we show how this works in perhaps the simplest example of GOE random matrices with a shifted diagonal. In the final subsection we describe how to extend this method to condition on the presence of a pseudogap at the bottom on the spectrum.

### A. The general method

Consider an  $N \times N$  real symmetric matrix  $A$ . An arbitrary function  $g$  of the minimum eigenvalue of  $A$  can be expressed using integrals over  $\mathbf{s} \in \mathbb{R}^N$  as

$$g(\lambda_{\min}(A)) = \lim_{\beta \rightarrow \infty} \int \frac{d\mathbf{s} \delta(N - \|\mathbf{s}\|^2) e^{-\beta \mathbf{s}^T A \mathbf{s}}}{\int d\mathbf{s}' \delta(N - \|\mathbf{s}'\|^2) e^{-\beta \mathbf{s}'^T A \mathbf{s}'}} g\left(\frac{\mathbf{s}^T A \mathbf{s}}{N}\right). \quad (1)$$

In the limit of large  $\beta$ , each integral concentrates among vectors  $\mathbf{s}$  in the eigenspace of  $A$  corresponding to the smallest eigenvalue of  $A$ . This produces

$$\begin{aligned} \lim_{\beta \rightarrow \infty} \int \frac{d\mathbf{s} \delta(N - \|\mathbf{s}\|^2) e^{-\beta \mathbf{s}^T A \mathbf{s}}}{\int d\mathbf{s}' \delta(N - \|\mathbf{s}'\|^2) e^{-\beta \mathbf{s}'^T A \mathbf{s}'}} g\left(\frac{\mathbf{s}^T A \mathbf{s}}{N}\right) &= \int \frac{d\mathbf{s} \delta(N - \|\mathbf{s}\|^2) \mathbb{1}_{\ker(A - \lambda_{\min}(A)I)}(\mathbf{s})}{\int d\mathbf{s}' \delta(N - \|\mathbf{s}'\|^2) \mathbb{1}_{\ker(A - \lambda_{\min}(A)I)}(\mathbf{s}')} g\left(\frac{\mathbf{s}^T A \mathbf{s}}{N}\right) \\ &= g(\lambda_{\min}(A)) \frac{\int d\mathbf{s} \delta(N - \|\mathbf{s}\|^2) \mathbb{1}_{\ker(A - \lambda_{\min}(A)I)}(\mathbf{s})}{\int d\mathbf{s}' \delta(N - \|\mathbf{s}'\|^2) \mathbb{1}_{\ker(A - \lambda_{\min}(A)I)}(\mathbf{s}')} \\ &= g(\lambda_{\min}(A)), \end{aligned} \quad (2)$$

as desired. The first relation extends a technique for calculating the typical minimum eigenvalue of an ensemble of matrices first introduced by Ikeda and later used by Kent-Dobias in the context of random landscapes and is similar to an earlier technique for conditioning the value of the ground state energy in random landscapes by Fyodorov and Le Doussal [21,22,24,25]. A Boltzmann distribution is introduced over a spherical model whose Hamiltonian is quadratic with interaction matrix given by  $A$ . In the limit of zero temperature, the measure will concentrate on the ground states of the model, which correspond with the eigenspace of  $A$  associated with its minimum eigenvalue  $\lambda_{\min}$ . The second relation uses the fact that, once restricted to the sphere  $\|\mathbf{s}\|^2 = N$  and the minimum eigenspace,  $\mathbf{s}^T A \mathbf{s} = \mathbf{s}^T \lambda_{\min}(A) \mathbf{s} = N \lambda_{\min}(A)$ .

The relationship is formal, but we can make use of the fact that the integral expression with a Gibbs distribution can be manipulated with replica techniques, averaged over, and in general treated with a physicist's toolkit. In particular, we have specific interest in using  $g(\lambda_{\min}(A)) = \delta(\lambda_{\min}(A))$ , a Dirac delta function, which can be inserted into averages over ensembles of matrices  $A$  (or indeed more complicated averages) in order to create the condition that the minimum eigenvalue is zero.

### B. Simple example: Shifted Gaussian orthogonal ensemble

We demonstrate the efficacy of the technique by rederiving a well-known result: the large-deviation function for pulling an eigenvalue from the bulk of the GOE spectrum. Consider an ensemble of  $N \times N$  matrices  $A = B + \mu I$  for  $B$  drawn from the GOE ensemble with entries whose variance is  $\sigma^2/N$ . We know that the bulk spectrum of  $A$  is a Wigner semicircle with radius  $2\sigma$  shifted by a constant  $\mu$ . Therefore, for  $\mu = 2\sigma$ , the minimum eigenvalue will typically be zero, while for  $\mu > 2\sigma$  the minimum eigenvalue would need to be a large deviation from the typical spectrum and its likelihood will be exponentially suppressed with  $N$ . For  $\mu < 2\sigma$ , the bulk of the typical spectrum contains zero and therefore a larger  $N^2$  deviation, moving an extensive number of eigenvalues, would be necessary [26]. This final case cannot be quantified by this method, but instead the nonexistence of a large deviation linear in  $N$  appears as the emergence of an imaginary part in the large deviation function.

To compute this large deviation function, we employ the method outlined in the previous subsection to calculate

$$\begin{aligned} e^{NG_{\lambda^*}(\mu)} &= P(\lambda_{\min}(B + \mu I) = \lambda^*) \\ &= \overline{\delta(N\lambda^* - N\lambda_{\min}(B + \mu I))}, \end{aligned} \quad (3)$$

169 where the overline is the average over  $B$ , and we have defined the large-deviation function  $G_{\lambda^*}(\mu)$ . Using the representation of  
 170  $\lambda_{\min}$  defined in (1), we have

$$e^{NG_{\lambda^*}(\mu)} = \lim_{\beta \rightarrow \infty} \int \frac{d\mathbf{s} \delta(N - \|\mathbf{s}\|^2) e^{-\beta \mathbf{s}^T (B + \mu I) \mathbf{s}}}{\int d\mathbf{s}' \delta(N - \|\mathbf{s}'\|^2) e^{-\beta \mathbf{s}'^T (B + \mu I) \mathbf{s}'}} \delta(N\lambda^* - \mathbf{s}^T (B + \mu I) \mathbf{s}), \quad (4)$$

171 Using replicas to treat the denominator ( $x^{-1} = \lim_{m \rightarrow 0} x^{m-1}$ ) and transforming the  $\delta$  function to its Fourier representation, we  
 172 have

$$e^{NG_{\lambda^*}(\mu)} = \lim_{\beta \rightarrow \infty} \lim_{m \rightarrow 0} \int d\hat{\lambda} \prod_{\alpha=1}^m [d\mathbf{s}^\alpha \delta(N - \|\mathbf{s}^\alpha\|^2)] \exp \left\{ -\beta \sum_{\alpha=1}^m (\mathbf{s}^\alpha)^T (B + \mu I) \mathbf{s}^\alpha + \hat{\lambda} [N\lambda^* - (\mathbf{s}^1)^T (B + \mu I) \mathbf{s}^1] \right\}, \quad (5)$$

173 having introduced the auxiliary parameter  $\hat{\lambda}$  in the Fourier representation of the  $\delta$  function. The whole expression, so transformed,  
 174 is an exponential integral linear in the matrix  $B$ . Taking the average over  $B$ , we find

$$e^{NG_{\lambda^*}(\mu)} = \lim_{\beta \rightarrow \infty} \lim_{m \rightarrow 0} \int d\hat{\lambda} \prod_{\alpha=1}^m [d\mathbf{s}^\alpha \delta(N - \|\mathbf{s}^\alpha\|^2)] \times \exp \left\{ N[\hat{\lambda}(\lambda^* - \mu) - m\beta\mu] + \frac{\sigma^2}{N} \left[ \beta^2 \sum_{\alpha\gamma} (\mathbf{s}^\alpha \cdot \mathbf{s}^\gamma)^2 + 2\beta\hat{\lambda} \sum_{\alpha} (\mathbf{s}^\alpha \cdot \mathbf{s}^1)^2 + \hat{\lambda}^2 N^2 \right] \right\}. \quad (6)$$

175 We make the Hubbard–Stratonovich transformation to the matrix field  $Q^{\alpha\beta} = \frac{1}{N} \mathbf{s}^\alpha \cdot \mathbf{s}^\beta$ . This produces an integral expression of  
 176 the form

$$e^{NG_{\lambda^*}(\mu)} = \lim_{\beta \rightarrow \infty} \lim_{m \rightarrow 0} \int d\hat{\lambda} dQ e^{N\mathcal{U}_{\text{GOE}}(\hat{\lambda}, Q|\beta, \lambda^*, \mu)}, \quad (7)$$

177 where the effective action  $\mathcal{U}_{\text{GOE}}$  is given by

$$\mathcal{U}_{\text{GOE}}(\hat{\lambda}, Q|\beta, \lambda^*, \mu) = \hat{\lambda}(\lambda^* - \mu) + \lim_{m \rightarrow 0} \left\{ -m\beta\mu + \sigma^2 \left[ \beta^2 \sum_{\alpha\gamma} (Q^{\alpha\gamma})^2 + 2\beta\hat{\lambda} \sum_{\alpha} (Q^{1\alpha})^2 + \hat{\lambda}^2 \right] + \frac{1}{2} \log \det Q \right\}, \quad (8)$$

178 and  $Q^{\alpha\alpha} = 1$  because of the spherical constraint. We can  
 179 evaluate this integral using the saddle-point method. We make  
 180 a replica symmetric ansatz for  $Q$ , because this is a 2-spin  
 181 spherical model but with the first row singled out because of  
 182 its unique coupling with  $\hat{\lambda}$ . The resulting matrix has the form

$$Q = \begin{bmatrix} 1 & \tilde{q}_0 & \tilde{q}_0 & \cdots & \tilde{q}_0 \\ \tilde{q}_0 & 1 & q_0 & \cdots & q_0 \\ \tilde{q}_0 & q_0 & 1 & \ddots & q_0 \\ \vdots & \vdots & \ddots & \ddots & \vdots \\ \tilde{q}_0 & q_0 & q_0 & \cdots & 1 \end{bmatrix}. \quad (9)$$

183 The relevant expressions in the effective action produce

$$\sum_{\alpha\beta} (Q^{\alpha\beta})^2 = m + 2(m-1)\tilde{q}_0^2 + (m-1)(m-2)q_0^2, \quad (10)$$

$$\sum_{\alpha} (Q^{1\alpha})^2 = 1 + (m-1)\tilde{q}_0^2, \quad (11)$$

$$\log \det Q = (m-2) \log(1 - q_0) + \log [1 + (m-2)q_0 - (m-1)\tilde{q}_0^2]. \quad (12)$$

184 Inserting these expressions into the effective action and taking  
 185 the limit of  $m$  to zero, we arrive at

$$e^{NG_{\lambda^*}(\mu)} = \lim_{\beta \rightarrow \infty} \int d\hat{\lambda} dq_0 d\tilde{q}_0 e^{N\mathcal{U}_{\text{GOE}}(\hat{\lambda}, q_0, \tilde{q}_0|\beta, \lambda^*, \mu)}, \quad (13)$$

with the new effective action

$$\mathcal{U}_{\text{GOE}}(\hat{\lambda}, q_0, \tilde{q}_0|\beta, \lambda^*, \mu) = \hat{\lambda}(\lambda^* - \mu) + \sigma^2 [2\beta^2(q_0^2 - \tilde{q}_0^2) + 2\beta\hat{\lambda}(1 - \tilde{q}_0^2) + \hat{\lambda}^2] - \log(1 - q_0) + \frac{1}{2} \log(1 - 2q_0 + \tilde{q}_0^2). \quad (14)$$

We need to evaluate the integral above using the saddle-point  
 187 method, but in the limit  $\beta \rightarrow \infty$ . We expect the overlaps to  
 188 concentrate on one as  $\beta$  goes to infinity. We therefore take  
 189

$$q_0 = 1 - y\beta^{-1} - z\beta^{-2} + O(\beta^{-3}), \quad (15)$$

$$\tilde{q}_0 = 1 - \tilde{y}\beta^{-1} - (z + \Delta z)\beta^{-2} + O(\beta^{-3}). \quad (16)$$

However, taking the limit with  $y \neq \tilde{y}$  results in an expression  
 190 for the action that diverges with  $\beta$ . To cure this, we must take  
 191  $\tilde{y} = y$ . The result is  
 192

$$\mathcal{U}_{\text{GOE}}(\hat{\lambda}, y, \Delta z|\infty, \lambda^*, \mu) = \hat{\lambda}(\lambda^* - \mu) + \sigma^2 [\hat{\lambda}^2 + 4(y + \Delta z)] + \frac{1}{2} \log \left( 1 - \frac{2\Delta z}{y^2} \right). \quad (17)$$

Extremizing this action over the new parameters  $y$ ,  $\Delta z$ , and  $\hat{\lambda}$ ,  
 193 we find  
 194

$$\hat{\lambda} = \frac{1}{\sigma} \sqrt{\left( \frac{\mu - \lambda^*}{2\sigma} \right)^2 - 1}, \quad (18)$$

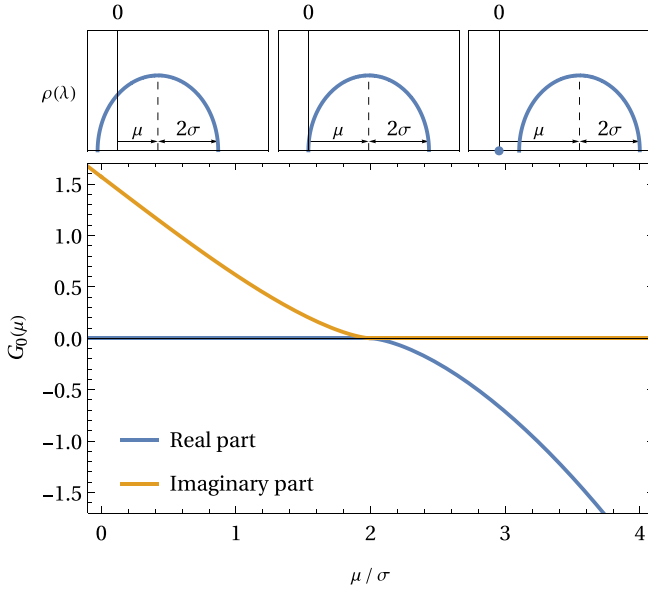


FIG. 1. The large deviation function  $G_0(\mu)$  defined in (3) as a function of the shift  $\mu$  to the GOE diagonal.  $G_0(2\sigma) = 0$ , while for  $\mu > 2\sigma$  it is negative and for  $\mu < 2\sigma$  it gains an imaginary part. The top panels show schematically what happens to the spectral density in each of these regimes. For  $\mu < 2\sigma$ , an  $N^2$ -large deviation would be required to fix the smallest eigenvalue to zero and the calculation breaks down, leading to the imaginary part. For  $\mu > 2\sigma$  the spectrum can satisfy the constraint on the smallest eigenvalue by isolating a single eigenvalue at zero at the cost of an order- $N$ -large deviation. At the transition point  $\mu = 2\sigma$  the spectrum is pseudogapped.

$$y = \frac{1}{2\sigma} \left[ \frac{\mu - \lambda^*}{2\sigma} + \sqrt{\left(\frac{\mu - \lambda^*}{2\sigma}\right)^2 - 1} \right]^{-1}, \quad (19)$$

$$\Delta z = \frac{1}{4\sigma^2} \left[ \left(\frac{\mu - \lambda^*}{2\sigma}\right)^2 - 1 - \frac{\mu - \lambda^*}{2\sigma} \sqrt{\left(\frac{\mu - \lambda^*}{2\sigma}\right)^2 - 1} \right]. \quad (20)$$

195 Inserting this solution into the effective action we arrive at

$$\begin{aligned} G_{\lambda^*}(\mu) &= \text{extremum}_{\hat{\lambda}, y, \Delta z} \mathcal{U}_{\text{GOE}}(\hat{\lambda}, y, \Delta z | \infty, \lambda^*, \mu) \\ &= -\frac{\mu - \lambda^*}{2\sigma} \sqrt{\left(\frac{\mu - \lambda^*}{2\sigma}\right)^2 - 1} \\ &\quad - \log \left[ \frac{\mu - \lambda^*}{2\sigma} - \sqrt{\left(\frac{\mu - \lambda^*}{2\sigma}\right)^2 - 1} \right]. \quad (21) \end{aligned}$$

196 This function is plotted in Fig. 1 for  $\lambda^* = 0$ . For  $\mu < 2\sigma$ ,  
 197  $G_0(\mu)$  has an imaginary part. This indicates that the existence  
 198 of a zero minimum eigenvalue when  $\mu < 2\sigma$  corresponds to a  
 199 large deviation that grows faster than  $N$ , rather like  $N^2$ , since  
 200 in this regime the bulk of the typical spectrum is over zero  
 201 and therefore extensively many eigenvalues must have large  
 202 deviations in order for the smallest eigenvalue to be zero [26].  
 203 For  $\mu \geq 2\sigma$  this function gives the large deviation function for

the probability of seeing a zero eigenvalue given the shift  $\mu$ .  
 $\mu = 2\sigma$  is the maximum of the function with a real value and  
 corresponds to the intersection of the typical bulk spectrum  
 with zero, i.e., a pseudogap.

Here, we see what appears to be a general heuristic for  
 identifying the saddle parameters for which the spectrum is  
 pseudogapped: the equivalent of this large-deviation function  
 will lie on the singular boundary between a purely real and  
 complex value.

### C. Conditioning on a pseudogap

We have seen that this method effectively conditions a  
 random matrix ensemble on its lowest eigenvalue being zero.  
 However, this does not correspond on its own to marginality.  
 In the previous example, most values of  $\mu$  where the calculation  
 was valid correspond to matrices with a single isolated  
 eigenvalue. However, the marginal minima we are concerned  
 with have pseudogapped spectra, where the continuous part of  
 the spectral density has a lower bound at zero.

Fortunately, our calculation can be modified to ensure that  
 we consider only pseudogapped spectra. First, we insert a shift  
 $\mu$  by hand into the “natural” spectrum of the problem at hand,  
 conditioning the trace to have a specific value  $\mu = \frac{1}{N} \text{Tr} A$ .  
 Then, we choose this artificial shift so that the resulting  
 conditioned spectra are pseudogapped. As seen in the previous  
 subsection, this can be done by starting from a sufficiently  
 large  $\mu$  and decreasing it until the calculation develops an  
 imaginary part, signaling the breakdown of the large-deviation  
 principle at order  $N$ .

In isotropic or zero-signal landscapes, there is another way  
 to condition on a pseudogap. In such landscapes, the typical  
 spectrum does not have an isolated eigenvalue. Therefore,  
 for a given  $\mu$  the bottom of the spectrum can be located by  
 looking for the value  $\lambda^*$  that maximizes the (real) large deviation  
 function. Inverting this reasoning, we can find the value  
 $\mu = \mu_m$  corresponding to a marginal spectrum by requiring  
 that the large deviation function has a maximum in  $\lambda^*$  at  
 $\lambda^* = 0$ , or

$$0 = \left. \frac{\partial}{\partial \lambda^*} G_{\lambda^*}(\mu_m) \right|_{\lambda^*=0}. \quad (22)$$

In the example problem of Sec. II B, this corresponds precisely  
 to  $\mu_m = 2\sigma$ , the correct marginal shift. Note that when  
 we treat the Dirac  $\delta$  function using its Fourier representation  
 with auxiliary parameter  $\hat{\lambda}$ , as in the previous subsection, this  
 condition corresponds with choosing  $\mu$  such that  $\hat{\lambda} = 0$ .

## III. MARGINAL COMPLEXITY IN RANDOM LANDSCAPES

The methods of the previous section can be used in diverse  
 settings. However, we are interested in applying them to study  
 stationary points in random landscapes whose Hessian spectrum  
 has a pseudogap; that is, that are marginal. In Sec. III A  
 we define the marginal complexity using the tools of the previous  
 section. In Sec. III B we review several general features in  
 a physicist’s approach to computing the marginal complexity.  
 In Sec. III C we introduce a representation of the marginal  
 complexity in terms of an integral over a superspace, which

condenses the notation and the resulting calculation and which we will use in one of our examples in the next section.

**A. Marginal complexity from Kac–Rice**

The situation in the study of random landscapes is often as follows: an ensemble of smooth energy functions  $H : \mathbb{R}^N \rightarrow \mathbb{R}$  defines a family of random landscapes, often with their configuration space subject to one or more constraints of the form  $g(\mathbf{x}) = 0$  for  $\mathbf{x} \in \mathbb{R}^N$ . The typical geometry of landscapes drawn from the ensemble is studied by their complexity, or the average logarithm of the number of stationary points with certain properties, e.g., of marginal minima at a given energy.

Such problems can be studied using the method of Lagrange multipliers, with one introduced for every constraint. If the configuration space is defined by  $r$  constraints, then the problem of identifying stationary points is reduced to extremizing the Lagrangian

$$L(\mathbf{x}, \omega) = H(\mathbf{x}) + \sum_{i=1}^r \omega_i g_i(\mathbf{x}) \quad (23)$$

with respect to  $\mathbf{x}$  and the Lagrange multipliers  $\omega = \{\omega_1, \dots, \omega_r\}$ . To write the gradient and Hessian of the energy, which are necessary to count stationary points, care must be taken to ensure they are constrained to the tangent space of the configuration manifold. For our purposes, the Lagrangian formalism offers a solution: the gradient  $\nabla H : \mathbb{R}^N \times \mathbb{R}^r \rightarrow \mathbb{R}^N$  and Hessian  $\text{Hess } H : \mathbb{R}^N \times \mathbb{R}^r \rightarrow \mathbb{R}^{N \times N}$  of the energy  $H$  can be written as the simple vector derivatives of the Lagrangian  $L$ , with

$$\nabla H(\mathbf{x}, \omega) = \partial L(\mathbf{x}, \omega) = \partial H(\mathbf{x}) + \sum_{i=1}^r \omega_i \partial g_i(\mathbf{x}), \quad (24)$$

$$\begin{aligned} \text{Hess } H(\mathbf{x}, \omega) &= \partial \partial L(\mathbf{x}, \omega) \\ &= \partial \partial H(\mathbf{x}) + \sum_{i=1}^r \omega_i \partial \partial g_i(\mathbf{x}), \end{aligned} \quad (25)$$

where  $\partial = \frac{\partial}{\partial \mathbf{x}}$  will always represent the derivative with respect to the vector argument  $\mathbf{x}$ . Note that, unlike the energy, which is a function of the configuration  $\mathbf{x}$  alone, the gradient and Hessian depend also on the Lagrange multipliers  $\omega$ . In situations with an extensive number of constraints, it is important to take seriously contributions of the form  $\frac{\partial^2 L}{\partial \mathbf{x} \partial \omega}$  to the Hessian [27]. However, the cases we study here have  $N^0$  constraints and these contributions appear as finite- $N$  corrections.

The number of stationary points in a landscape for a particular function  $H$  is found by integrating over the Kac–Rice measure

$$\begin{aligned} dv_H(\mathbf{x}, \omega) &= d\mathbf{x} d\omega \delta(\mathbf{g}(\mathbf{x})) \delta(\nabla H(\mathbf{x}, \omega)) \\ &\quad \times |\det \text{Hess } H(\mathbf{x}, \omega)|, \end{aligned} \quad (26)$$

with a  $\delta$  function of the gradient and the constraints ensuring that we count valid stationary points, and the determinant of the Hessian serving as the Jacobian of the argument to the  $\delta$  function [28,29]. It is usually more interesting to condition the count on interesting properties of the stationary points, such as the energy and spectrum trace, or

$$\begin{aligned} dv_H(\mathbf{x}, \omega | E, \mu) &= dv_H(\mathbf{x}, \omega) \delta(NE - H(\mathbf{x})) \\ &\quad \times \delta(N\mu - \text{Tr Hess } H(\mathbf{x}, \omega)). \end{aligned} \quad (27)$$

We specifically want to control the value of the minimum eigenvalue of the Hessian at the stationary points. Using the method introduced in Sec. II, we can write the number of stationary points with energy  $E$ , the Hessian trace  $\mu$ , and the smallest eigenvalue  $\lambda^*$  as

$$\begin{aligned} \mathcal{N}_H(E, \mu, \lambda^*) &= \int dv_H(\mathbf{x}, \omega | E, \mu) \delta(N\lambda^* - \lambda_{\min}(\text{Hess } H(\mathbf{x}, \omega))) \\ &= \lim_{\beta \rightarrow \infty} \int dv_H(\mathbf{x}, \omega | E, \mu) \frac{\int ds \delta(N - \|s\|^2) \delta(s^T \partial \mathbf{g}(\mathbf{x})) e^{-\beta s^T \text{Hess } H(\mathbf{x}, \omega) s}}{\int ds' \delta(N - \|s'\|^2) \delta(s'^T \partial \mathbf{g}(\mathbf{x})) e^{-\beta s'^T \text{Hess } H(\mathbf{x}, \omega) s'}} \delta(N\lambda^* - s^T \text{Hess } H(\mathbf{x}, \omega) s), \end{aligned} \quad (28)$$

where the additional  $\delta$  functions

$$\delta(s^T \partial \mathbf{g}(\mathbf{x})) = \prod_{s=1}^r \delta(s^T \partial g_s(\mathbf{x})) \quad (29)$$

ensure that the integrals involving potential eigenvectors  $s$  are constrained to the tangent space of the configuration manifold at the point  $\mathbf{x}$ .

The complexity of points with a specific energy, stability, and minimum eigenvalue is defined as the average over the ensemble of functions  $H$  of the logarithm of the number  $\mathcal{N}_H$  of stationary points, or

$$\Sigma_{\lambda^*}(E, \mu) = \frac{1}{N} \overline{\log \mathcal{N}_H(E, \mu, \lambda^*)}. \quad (30)$$

In practice, this can be computed by introducing replicas to treat the logarithm ( $\log x = \lim_{n \rightarrow 0} \frac{\partial}{\partial n} x^n$ ) and introducing another set of replicas to treat each of the normalizations in the numerator ( $x^{-1} = \lim_{m \rightarrow -1} x^m$ ). This leads to the

311 expression

$$\begin{aligned} \Sigma_{\lambda^*}(E, \mu) = & \lim_{\beta \rightarrow \infty} \lim_{n \rightarrow 0} \frac{1}{N} \frac{\partial}{\partial n} \int \prod_{a=1}^n \left[ d\nu_H(\mathbf{x}_a, \omega_a | E, \mu) \delta(N\lambda^* - (\mathbf{s}_a^1)^T \text{Hess} H(\mathbf{x}_a, \omega_a) \mathbf{s}_a^1) \right. \\ & \left. \times \lim_{m_a \rightarrow 0} \left( \prod_{\alpha=1}^{m_a} d\mathbf{s}_a^\alpha \delta(N - \|\mathbf{s}_a^\alpha\|^2) \delta((\mathbf{s}_a^\alpha)^T \partial \mathbf{g}(\mathbf{x}_a)) e^{-\beta(\mathbf{s}_a^\alpha)^T \text{Hess} H(\mathbf{x}_a, \omega_a) \mathbf{s}_a^\alpha} \right) \right] \end{aligned} \quad (31)$$

312 for the complexity of stationary points of a given energy, trace,  
313 and smallest eigenvalue.

314 The marginal complexity follows from the complexity as  
315 a function of  $\mu$  and  $\lambda^*$  in an analogous way to Sec. II C. In  
316 general, one sets  $\lambda^* = 0$  and tunes  $\mu$  from a sufficiently large  
317 value until the complexity develops an imaginary component,  
318 which corresponds to the bulk of the spectrum touching zero.  
319 The value  $\mu = \mu_m$  that satisfies this is the marginal stability.

320 In the cases studied here with zero signal to noise, a simpler  
321 approach is possible. The marginal stability  $\mu = \mu_m$  can be  
322 identified by requiring that the complexity is stationary with  
323 respect to changes in the value of the minimum eigenvalue  $\lambda^*$ ,  
324 or

$$0 = \frac{\partial}{\partial \lambda^*} \Sigma_{\lambda^*}(E, \mu_m(E)) \Big|_{\lambda^*=0}. \quad (32)$$

325 The marginal complexity follows by evaluating the com-  
326 plexity conditioned on  $\lambda^* = 0$  at the marginal stability  $\mu =$   
327  $\mu_m(E)$ ,

$$\Sigma_m(E) = \Sigma_0(E, \mu_m(E)). \quad (33)$$

### 328 B. General features of saddle-point computation

329 Several elements of the computation of the marginal com-  
330 plexity, and indeed the ordinary dominant complexity, follow  
331 from the formulas of the above section in the same way. The  
332 physicist's approach to this problem seeks to convert all of the  
333 components of the Kac–Rice measure defined in (26) and (27)  
334 into elements of an exponential integral over configuration  
335 space. To begin with, all Dirac  $\delta$  functions are expressed using  
336 their Fourier representation, with

$$\delta(\nabla H(\mathbf{x}_a, \omega_a)) = \int \frac{d\hat{\mathbf{x}}_a}{(2\pi)^N} e^{i\hat{\mathbf{x}}_a^T \nabla H(\mathbf{x}_a, \omega_a)}, \quad (34)$$

$$\delta(NE - H(\mathbf{x}_a)) = \int \frac{d\hat{\beta}_a}{2\pi} e^{\hat{\beta}_a [NE - H(\mathbf{x}_a)]}, \quad (35)$$

$$\begin{aligned} \delta(N\lambda^* - (\mathbf{s}_a^1)^T \text{Hess} H(\mathbf{x}_a, \omega) \mathbf{s}_a^1) \\ = \int \frac{d\hat{\lambda}_a}{2\pi} e^{\hat{\lambda}_a [N\lambda^* - (\mathbf{s}_a^1)^T \text{Hess} H(\mathbf{x}_a, \omega) \mathbf{s}_a^1]}. \end{aligned} \quad (36)$$

337 To do this we introduced auxiliary fields  $\hat{\mathbf{x}}_a$ ,  $\hat{\beta}_a$ , and  $\hat{\lambda}_a$ .  
338 Because the permutation symmetry of replica vectors is pre-  
339 served in replica symmetry breaking (RSB) orders, the order  
340 parameters  $\beta$  and  $\lambda$  will quickly lose their indices, since they  
341 will ubiquitously be constant over the replica index at the  
342 eventual saddle-point solution.

343 We would like to make a similar treatment of the de-  
344 terminant of the Hessian that appears in (26). The standard  
345 approach is to drop the absolute value function around the

determinant. This can potentially lead to severe problems with  
346 the complexity [19]. However, it is a justified step when the  
347 parameters of the problem  $E$ ,  $\mu$ , and  $\lambda^*$  put us in a regime  
348 where the exponential majority of stationary points have the  
349 same index. This is true for maxima and minima, and for  
350 saddle points whose spectra have a strictly positive bulk with  
351 a fixed number of negative outliers. It is in particular a safe  
352 operation for the present problem of marginal minima, which  
353 lie right at the edge of disaster.

354 Dropping the absolute value function allows us to write

$$\det \text{Hess} H(\mathbf{x}_a, \omega_a) = \int d\bar{\eta}_a d\eta_a e^{-\bar{\eta}_a^T \text{Hess} H(\mathbf{x}_a, \omega_a) \eta_a} \quad (37)$$

355 using the  $N$ -dimensional Grassmann vectors  $\bar{\eta}_a$  and  $\eta_a$ . For  
356 the spherical models this step is unnecessary, since there are  
357 other ways to treat the determinant keeping the absolute value  
358 signs, as in previous works [4,7]. However, other examples of  
359 ours are for models where the same techniques are impossible.

360 Finally, the  $\delta$  function fixing the trace of the Hessian to  $\mu$   
361 in (27) must be addressed. One could treat it using a Fourier  
362 representation as in (34)–(36), but this is inconvenient because  
363 a term of the form  $\text{Tr} \partial \partial H(\mathbf{x})$  in the exponential integrand  
364 cannot be neatly captured in superspace representation intro-  
365 duced in the next section. However, in the cases we study in  
366 this paper a simplification can be made: the trace of  $\partial \partial H$  can  
367 be separated into two pieces, one that is spatially independent  
368 and one that is typically small, or

$$\text{Tr} \partial \partial H(\mathbf{x}) = N\mu_H^* + \Delta_H(\mathbf{x}), \quad (38)$$

369 where  $\overline{\mu_H^*} = \mu^*$  and  $\overline{\Delta_H(\mathbf{x})} = O(N^0)$ . Then fixing the trace of  
370 the Hessian to  $\mu$  implies that

$$\begin{aligned} \mu &= \frac{1}{N} \text{Tr} \text{Hess} H(\mathbf{x}) = \frac{1}{N} \left( \partial \partial H(\mathbf{x}) + \sum_{i=1}^r \omega_i \text{Tr} \partial \partial g_i(\mathbf{x}) \right) \\ &= \mu^* + \frac{1}{N} \sum_{i=1}^r \omega_i \text{Tr} \partial \partial g_i(\mathbf{x}) + O(N^{-1}) \end{aligned} \quad (39)$$

372 for typical samples  $H$ . In particular, here we study only cases  
373 with quadratic  $g_i$ , which results in a linear expression relating  
374  $\mu$  and the  $\omega_i$  that is independent of  $\mathbf{x}$ . Since  $H$  contains the  
375 disorder of the problem, this simplification means that the  
376 effect of fixing the trace is largely independent of the disorder  
377 and mostly depends on properties of the constraint manifold.

### 378 C. Superspace representation

379 The ordinary Kac–Rice calculation involves many moving  
380 parts, and this method for incorporating marginality adds even  
381 more. It is therefore convenient to introduce compact and sim-

382 plifying notation through a superspace representation. The use  
 383 of superspace in the Kac–Rice calculation is well established,  
 384 as well as the deep connections with Becchi-Rouet-Stora-  
 385 Tyutin (BRST) symmetry that is implied [30–32]. Appendix A  
 386 introduces the notation and methods of superspace algebra.  
 387 Here we describe how it can be used to simplify the complex-  
 388 ity calculation for marginal minima.

389 We consider the  $\mathbb{R}^{N|4}$  superspace whose Grassmann indices  
 390 are  $\bar{\theta}_1, \theta_1, \bar{\theta}_2, \theta_2$ . Consider the supervector defined by

$$\phi_a^\alpha(1, 2) = \mathbf{x}_a + \bar{\theta}_1 \eta_a + \bar{\eta}_a \theta_1 + i \hat{\mathbf{x}}_a \bar{\theta}_1 \theta_1 + \mathbf{s}_a^\alpha (\bar{\theta}_1 \theta_2 + \bar{\theta}_2 \theta_1). \quad (40)$$

391 Note that this supervector does not span the whole superspace:  
 392 only a couple terms from the  $\bar{\theta}_2, \theta_2$  sector are present, since  
 393 the rest are unnecessary for our representation. With this su-  
 394 pervector so defined, the replicated count of stationary points  
 395 with energy  $E$ , trace  $\mu$ , and smallest eigenvalue  $\lambda^*$  can be  
 396 written as

$$\begin{aligned} \mathcal{N}_H(E, \mu, \lambda^*)^n &= \lim_{\beta \rightarrow \infty} \int d\omega d\hat{\beta} d\hat{\lambda} \prod_{a=1}^n \lim_{m_a \rightarrow 0} \prod_{\alpha=1}^{m_a} d\phi_a^\alpha \exp \left\{ \delta^{\alpha 1} N(\hat{\beta} E \right. \\ &\quad \left. + \hat{\lambda} \lambda^*) + \int d1 d2 B^\alpha(1, 2) L(\phi_a^\alpha(1, 2), \omega) \right\}. \end{aligned} \quad (41)$$

397 Here we have also defined the operator

$$B^\alpha(1, 2) = \delta^{\alpha 1} \bar{\theta}_2 \theta_2 (1 - \hat{\beta} \bar{\theta}_1 \theta_1) - \delta^{\alpha 1} \hat{\lambda} - \beta, \quad (42)$$

398 which encodes various aspects of the complexity problem.  
 399 When the Lagrangian is expanded in a series with respect to  
 400 the Grassmann indices and the definition of  $B$  inserted, the  
 401 result of the Grassmann integrals produces exactly the content  
 402 of the integrand in (31) with the substitutions (34), (35), (36),  
 403 and (37) of the Dirac  $\delta$  functions and the determinant made.  
 404 The new measures

$$d\phi_a^\alpha = \left[ d\mathbf{x}_a \delta(\mathbf{g}(\mathbf{x}_a)) \frac{d\hat{\mathbf{x}}_a}{(2\pi)^N} d\eta_a d\bar{\eta}_a \delta^{\alpha 1} + (1 - \delta^{\alpha 1}) \right] \\ \times d\mathbf{s}_a^\alpha \delta(\|\mathbf{s}_a^\alpha\|^2 - N) \delta((\mathbf{s}_a^\alpha)^T \partial \mathbf{g}(\mathbf{x}_a)), \quad (43)$$

$$d\omega = \left( \prod_{i=1}^r d\omega_i \right) \delta \left( N\mu - \mu^* - \sum_i \omega_i \text{Tr} \partial \partial g_i \right) \quad (44)$$

405 collect the individual measures of the various fields embed-  
 406 ded in the superfield, along with their constraints. With this  
 407 way of writing the replicated count, the problem of marginal  
 408 complexity temporarily takes the schematic form of an equi-  
 409 librium calculation with configurations  $\phi$ , inverse temperature  
 410  $B$ , and energy  $L$ . This makes the intermediate pieces of the  
 411 calculation dramatically simpler. Of course the intricacies of  
 412 the underlying problem are not banished: near the end of the  
 413 calculation, terms involving the superspace must be expanded.  
 414 We will make use of this representation to simplify the analy-

sis of the marginal complexity when analyzing random sums  
 of squares in Sec. IV C.

## IV. EXAMPLES

In this section we present analysis of marginal complexity  
 in three random landscapes. In Sec. IV A we treat the spherical  
 spin glasses, which reveals some general aspects of the calcula-  
 tion. Since the spherical spin glasses are Gaussian and have  
 identical GOE spectra at each stationary point, the approach  
 introduced here is overkill. In Sec. IV B we apply the methods  
 to a multispherical spin glass, which is still Gaussian but has a  
 non-GOE spectrum whose shape can vary between stationary  
 points. Finally, in Sec. IV C we analyze a model of sums of  
 squared random functions, which is non-Gaussian and whose  
 Hessian statistics depend on the conditioning of the energy  
 and gradient.

### A. Spherical spin glasses

The spherical spin glasses are a family of models that  
 encompass every isotropic Gaussian field on the hypersphere.  
 Their configuration space is the sphere  $S^{N-1}$  defined by all  
 $\mathbf{x} \in \mathbb{R}^N$  such that  $0 = g(\mathbf{x}) = \frac{1}{2}(\|\mathbf{x}\|^2 - N)$ . One can consider  
 the models as defined by ensembles of centered Gaussian  
 functions  $H$  such that the covariance between two points in  
 the configuration space is

$$\overline{H(\mathbf{x})H(\mathbf{x}')} = Nf\left(\frac{\mathbf{x} \cdot \mathbf{x}'}{N}\right) \quad (45)$$

for some function  $f$  with positive series coefficients. Such  
 functions can be considered to be made up of all-to-all ten-  
 sorial interactions, with

$$H(\mathbf{x}) = \sum_{p=0}^{\infty} \frac{1}{p!} \sqrt{\frac{f^{(p)}(0)}{N^{p-1}}} \sum_{i_1, \dots, i_p} J_{i_1, \dots, i_p} x_{i_1} \cdots x_{i_p}, \quad (46)$$

and the elements of the tensors  $J$  being independently dis-  
 tributed with the unit normal distribution [33]. We focus on  
 marginal minima in models with  $f'(0) = 0$ , which corre-  
 sponds to models without a random external field. Such a  
 random field would correspond in each individual sample  $H$  to  
 a signal, and therefore complicate the analysis by correlating  
 the positions of stationary points and the eigenvectors of their  
 Hessians. Here,  $\mu^*$  of (38) is zero.

The marginal optima of these models can be studied with-  
 out the methods introduced in this paper, and have been in  
 the past [4,7]. First, these models are Gaussian, so at large  
 $N$  the Hessian is statistically independent of the gradient and  
 energy [19,20]. Therefore, conditioning the Hessian can be  
 done mostly independently from the problem of counting  
 stationary points. Second, in these models the Hessian at every  
 point in the landscape belongs to the GOE class with the same  
 width of the spectrum  $\mu_m = 2\sqrt{f''(1)}$ . Therefore, all marginal  
 minima in these systems have the same constant shift  $\mu = \mu_m$ .  
 Despite the fact that the complexity of marginal optima is well  
 known by simpler methods, it is instructive to carry through  
 the calculation for this case, since we will learn some things  
 about its application in more nontrivial settings.

Note that in the pure version of these models with  $f(q) = \frac{1}{2}q^p$ , the methods of this section must be amended slightly. This is because in these models there is an exact correspondence  $\mu = -pE$  between the trace of the Hessian and the energy, and therefore they cannot be fixed independently. This correspondence implies that when  $\mu = \mu_m$ , the corresponding energy level  $E_{\text{th}} = -\frac{1}{p}\mu_m$  contains all marginal minima. This is what gives this threshold energy such singular importance to dynamics in the pure spherical models.

The procedure to treat the complexity of the spherical models has been made in detail elsewhere [7]. Here we make only a sketch of the steps involved. First we notice that  $\mu = \frac{1}{N}\omega \text{Tr} \partial \partial g(\mathbf{x}) = \omega$ , so that the only Lagrange multiplier  $\omega$  in this problem is set directly to the shift  $\mu$ . The substitutions (34), (35), and (36) are made to convert the Dirac  $\delta$  functions into exponential integrals, and the substitution (37) is made to likewise convert the determinant.

Once these substitutions have been made, the entire expression (31) is an exponential integral whose argument is a linear functional of  $H$ . This allows for the average to be taken over the disorder. If we gather all the  $H$ -dependant pieces associated with replica  $a$  into the linear functional  $\mathcal{O}_a$  then

the average over the ensemble of functions  $H$  gives

$$\begin{aligned}
 \overline{e^{\sum_a^n \mathcal{O}_a H(\mathbf{x}_a)}} &= e^{\frac{1}{2} \sum_a^n \sum_b^n \mathcal{O}_a \mathcal{O}_b \overline{H(\mathbf{x}_a)H(\mathbf{x}_b)}} \\
 &= e^{N \frac{1}{2} \sum_a^n \sum_b^n \mathcal{O}_a \mathcal{O}_b f(\frac{\mathbf{x}_a \cdot \mathbf{x}_b}{N})}.
 \end{aligned} \tag{47}$$

The result is an integrand that depends on the many vector variables we have introduced only through their scalar products with each other. We therefore make a change of variables in the integration from those vectors to matrices that encode their possible scalar products. These matrices are

$$\begin{aligned}
 C_{ab} &= \frac{1}{N} \mathbf{x}_a \cdot \mathbf{x}_b, & R_{ab} &= -i \frac{1}{N} \mathbf{x}_a \cdot \hat{\mathbf{x}}_b, & D_{ab} &= \frac{1}{N} \hat{\mathbf{x}}_a \cdot \hat{\mathbf{x}}_b, \\
 Q_{ab}^{\alpha\gamma} &= \frac{1}{N} \mathbf{s}_a^\alpha \cdot \mathbf{s}_b^\gamma, & \hat{X}_{ab}^\alpha &= -i \frac{1}{N} \hat{\mathbf{x}}_a \cdot \mathbf{s}_b^\alpha, & X_{ab}^\alpha &= \frac{1}{N} \mathbf{x}_a \cdot \mathbf{s}_b^\alpha, \\
 G_{ab} &= \frac{1}{N} \bar{\eta}_a \cdot \eta_b.
 \end{aligned} \tag{48}$$

Order parameters that mix the normal and Grassmann variables generically vanish in these settings and we don't consider them here [34]. This transformation changes the measure of the integral, with

$$\prod_{a=1}^n d\mathbf{x}_a \frac{d\hat{\mathbf{x}}_a}{(2\pi)^N} d\bar{\eta}_a d\eta_a \prod_{\alpha=1}^{m_a} d\mathbf{s}_a^\alpha = dC dR dD dG dQ dX d\hat{X} (\det J)^{N/2} (\det G)^{-N}, \tag{49}$$

where  $J$  is the Jacobian of the transformation in the real-valued fields. This Jacobian takes a block form

$$J = \begin{bmatrix} C & iR & X_1 & \cdots & X_n \\ iR & D & i\hat{X}_1 & \cdots & i\hat{X}_n \\ X_1^T & i\hat{X}_1^T & Q_{11} & \cdots & Q_{1n} \\ \vdots & \vdots & \vdots & \ddots & \vdots \\ X_n^T & i\hat{X}_n^T & Q_{n1} & \cdots & Q_{nn} \end{bmatrix}. \tag{50}$$

The Grassmann integrals produces their own inverted Jacobian. The matrix that make up the blocks of the matrix  $J$  are such that  $C$ ,  $R$ , and  $D$  are  $n \times n$  matrices indexed by their lower indices,  $Q_{ab}$  is an  $m_a \times m_b$  matrix indexed by its upper indices, while  $X_a$  is an  $n \times m_a$  matrix with one lower and one upper index.

These steps follow identically to those more carefully outlined in the cited papers [4,7]. Following them in the present case, we arrive at a form for the complexity of stationary points with fixed energy  $E$ , stability  $\mu$ , and lowest eigenvalue  $\lambda^*$  with

$$\begin{aligned}
 \Sigma_{\lambda^*}(E, \mu) &= \lim_{\beta \rightarrow \infty} \lim_{n \rightarrow 0} \lim_{m_1 \cdots m_n \rightarrow 0} \frac{1}{N} \frac{\partial}{\partial n} \int dC dR dD dG dQ dX d\hat{X} d\hat{\beta} d\hat{\lambda} \\
 &\times \exp \left\{ nN S_{\text{SSG}}(\hat{\beta}, C, R, D, G|E, \mu) + nN U_{\text{SSG}}(\hat{\lambda}, Q, X, \hat{X}|\beta, \lambda^*, \mu, C) \right. \\
 &\left. + \frac{N}{2} \log \det \left[ I - \begin{bmatrix} Q_{11} & \cdots & Q_{1n} \\ \vdots & \ddots & \vdots \\ Q_{n1} & \cdots & Q_{nn} \end{bmatrix}^{-1} \begin{bmatrix} X_1^T & i\hat{X}_1^T \\ \vdots & \vdots \\ X_n^T & i\hat{X}_n^T \end{bmatrix} \begin{bmatrix} C & iR \\ iR & D \end{bmatrix}^{-1} \begin{bmatrix} X_1 \cdots X_n \\ i\hat{X}_1 \cdots i\hat{X}_n \end{bmatrix} \right] \right\}.
 \end{aligned} \tag{51}$$

501 The exponential integrand is split into two effective actions coupled only by a residual determinant. The first of these actions is  
 502 the usual effective action for the complexity of the spherical spin glasses, or

$$\begin{aligned} S_{\text{SSG}}(\hat{\beta}, C, R, D, G|E, \mu) = & \hat{\beta}E + \lim_{n \rightarrow 0} \frac{1}{n} \left\{ -\mu \text{Tr}(R + G) + \frac{1}{2} \sum_{ab} [\hat{\beta}^2 f(C_{ab}) + (2\hat{\beta}R_{ab} - D_{ab})f'(C_{ab}) \right. \\ & \left. + (R_{ab}^2 - G_{ab}^2)f''(C_{ab})] + \frac{1}{2} \log \det \begin{bmatrix} C & iR \\ iR^T & D \end{bmatrix} - \log \det G \right\}. \end{aligned} \quad (52)$$

503 The second of these actions is analogous to the effective action (8) from the GOE example of Sec. IIB and contains the  
 504 contributions from the marginal pieces of the calculation, and is given by

$$\begin{aligned} \mathcal{U}_{\text{SSG}}(\hat{\lambda}, Q, X, \hat{X}|\beta, \lambda^*, \mu, C) \\ = & \hat{\lambda}\lambda^* + \lim_{n \rightarrow 0} \lim_{m_1 \dots m_n \rightarrow 0} \frac{1}{n} \left\{ \frac{1}{2} \log \det Q - \sum_{a=1}^n \left( \sum_{\alpha=1}^{m_a} \beta \mu Q_{aa}^{\alpha\alpha} + \hat{\lambda} \mu Q_{aa}^{11} \right) + 2 \sum_{ab}^n f''(C_{ab}) \right. \\ & \left. \times \left[ \beta \sum_{\alpha}^{m_a} \left( \beta \sum_{\gamma}^{m_b} (Q_{ab}^{\alpha\gamma})^2 - \hat{\beta} (X_{ab}^{\alpha})^2 - 2X_{ab}^{\alpha} \hat{X}_{ab}^{\alpha} \right) + \hat{\lambda} (\hat{\lambda} (Q_{ab}^{11})^2 - \hat{\beta} (X_{ab}^1)^2 - 2X_{ab}^1 \hat{X}_{ab}^1) + \beta \hat{\lambda} \left( \sum_{\alpha}^{m_a} Q_{ab}^{\alpha 1} + \sum_{\alpha}^{m_b} Q_{ab}^{1\alpha} \right) \right] \right\}. \end{aligned} \quad (53)$$

505 The fact that the complexity can be split into two relatively in-  
 506 dependent pieces in this way is a characteristic of the isotropic  
 507 and Gaussian nature of the spherical spin glass. In Sec. IVC  
 508 we study a model whose energy is isotropic but not Gaussian  
 509 and where such a decomposition is impossible.

510 There are some dramatic simplifications that emerge from  
 511 the structure of this particular problem. First, notice that the  
 512 dependence on the parameters  $X$  and  $\hat{X}$  are purely quadratic.  
 513 Therefore, there will always be a saddle-point condition where  
 514 they are both zero. In this case without a fixed or random field,  
 515 we expect this solution to be correct. We can reason about why  
 516 this is so:  $X$ , for instance, quantifies the correlation between  
 517 the typical position of stationary points and the direction of  
 518 their typical eigenvectors. In a landscape without a signal,  
 519 where no direction is any more important than any other, we  
 520 expect such correlations to be zero: where a state is located  
 521 does not give any information as to the orientation of its soft  
 522 directions. On the other hand, in the spiked case, or with an  
 523 external field, the preferred direction can polarize both the di-  
 524 rection of typical stationary points *and* their soft eigenvectors.  
 525 Therefore, in these instances one must account for solutions  
 526 with nonzero  $X$  and  $\hat{X}$ .

527 We similarly expect that  $Q_{ab} = 0$  for  $a \neq b$ . For the  
 528 contrary to be true, eigenvectors at independently sampled  
 529 stationary points would need to have their directions cor-  
 530 related. This is expected in situations with a signal, where  
 531 such correlations would be driven by a shared directional bias  
 532 towards the signal. In the present situation, where there is no  
 533 signal, such correlations do not exist.

534 When we take  $X = \hat{X} = 0$  and  $Q_{ab}^{\alpha\beta} = \delta_{ab} Q^{\alpha\beta}$ , we find that

$$\mathcal{U}_{\text{SSG}}(\hat{\lambda}, Q, 0, 0|\beta, \lambda^*, \mu, C) = \mathcal{U}_{\text{GOE}}(\hat{\lambda}, Q|\beta, \lambda^*, \mu), \quad (54)$$

535 with  $\sigma^2 = f''(1)$ . That is, the effective action for the terms  
 536 related to fixing the eigenvalue in the spherical Kac–Rice  
 537 problem is exactly the same as that for the GOE problem.  
 538 This is perhaps not so surprising, since we established from  
 539 the beginning that the Hessian of the spherical spin glasses  
 540 belongs to the GOE class.

The remaining analysis of the eigenvalue-dependent part  
 $\mathcal{U}_{\text{SSG}}$  follows precisely the same steps as were made in  
 Sec. IIB for the GOE example. The result of the calcula-  
 tion is also the same: the exponential factor containing  $\mathcal{U}_{\text{SSG}}$   
 produces precisely the large deviation function  $G_{\lambda^*}(\mu)$  of  
 (21) [again with  $\sigma^2 = f''(1)$ ]. The remainder of the inte-  
 grand depending on  $S_{\text{SSG}}$  produces the ordinary complexity  
 of the spherical spin glasses without conditions on the Hessian  
 eigenvalue. We therefore find that

$$\Sigma_{\lambda^*}(E, \mu) = \Sigma(E, \mu) + G_{\lambda^*}(\mu). \quad (55)$$

We find the marginal complexity by solving

$$0 = \frac{\partial}{\partial \lambda^*} \Sigma_{\lambda^*}(E, \mu_m(E)) \Big|_{\lambda^*=0} = \frac{\partial}{\partial \lambda^*} G_{\lambda^*}(\mu_m(E)) \Big|_{\lambda^*=0}, \quad (56)$$

551 which gives  $\mu_m(E) = 2\sigma = 2\sqrt{f''(1)}$  independent of  $E$ , as  
 552 we presaged above. Since  $G_0(\mu_m) = 0$ , this gives finally

$$\Sigma_m(E) = \Sigma_0(E, \mu_m(E)) = \Sigma(E, \mu_m). \quad (57)$$

553 The marginal complexity in these models is thus simply the  
 554 ordinary complexity evaluated at a fixed trace  $\mu_m$  of the Hes-  
 555 sian.

## B. Multispherical spin glasses

557 The multispherical spin glasses are a simple extension of  
 558 the spherical ones, where the configuration space is taken to  
 559 be the union of more than one hypersphere. Here we consider  
 560 the specific case where the configuration space is the union  
 561 of two  $(N-1)$ -spheres, with  $\Omega = S^{N-1} \times S^{N-1}$ . The two  
 562 spheres give rise to two constraints: for  $\mathbf{x} = [\mathbf{x}^{(1)}, \mathbf{x}^{(2)}]$  with  
 563 components  $\mathbf{x}^{(1)}, \mathbf{x}^{(2)} \in \mathbb{R}^N$ , the constraints are  $0 = g_1(\mathbf{x}) =$   
 564  $\frac{1}{2}(\|\mathbf{x}^{(1)}\|^2 - N)$  and  $0 = g_2(\mathbf{x}) = \frac{1}{2}(\|\mathbf{x}^{(2)}\|^2 - N)$ . These two  
 565 constraints are fixed by two Lagrange multipliers  $\omega_1$  and  $\omega_2$ .

The energy in our multispherical spin glass is given by

$$H(\mathbf{x}) = H_1(\mathbf{x}^{(1)}) + H_2(\mathbf{x}^{(2)}) - \epsilon \mathbf{x}^{(1)} \cdot \mathbf{x}^{(2)}. \quad (58)$$

567 The energy  $H_i$  of each individual sphere is taken to be a  
568 centered Gaussian random function with a covariance given  
569 in the usual spherical spin glass way for  $\mathbf{x}, \mathbf{x}' \in \mathbb{R}^N$  by

$$\overline{H_i(\mathbf{x})H_j(\mathbf{x}')} = N\delta_{ij}f_i\left(\frac{\mathbf{x} \cdot \mathbf{x}'}{N}\right), \quad (59)$$

570 with the functions  $f_1$  and  $f_2$  not necessarily the same. As for  
571 the spherical spin glasses,  $\mu^*$  of (38) is zero.

572 In this problem, there is an energetic competition between  
573 the independent spin glass energies on each sphere and their  
574 tendency to align or anti-align through the interaction term.  
575 These models have more often been studied with random  
576 fully connected couplings between the spheres, for which it is  
577 possible to also use configuration spaces involving spheres of  
578 different sizes [35–41]. The deterministically coupled model  
579 was previously studied as a thought experiment [7].

580 We again make use of the method of Lagrange multipliers  
581 to find stationary points on the constrained configuration  
582 space. The Lagrangian and its gradient and Hessian are

$$L(\mathbf{x}) = H(\mathbf{x}) + \frac{1}{2}\omega_1(\|\mathbf{x}^{(1)}\|^2 - N) + \frac{1}{2}\omega_2(\|\mathbf{x}^{(2)}\|^2 - N), \quad (60)$$

$$\nabla H(\mathbf{x}, \omega) = \begin{bmatrix} \partial_1 H_1(\mathbf{x}^{(1)}) - \epsilon \mathbf{x}^{(2)} + \omega_1 \mathbf{x}^{(1)} \\ \partial_2 H_2(\mathbf{x}^{(2)}) - \epsilon \mathbf{x}^{(1)} + \omega_2 \mathbf{x}^{(2)} \end{bmatrix}, \quad (61)$$

$$\text{Hess } H(\mathbf{x}, \omega) = \begin{bmatrix} \partial_1 \partial_1 H_1(\mathbf{x}^{(1)}) + \omega_1 I & -\epsilon I \\ -\epsilon I & \partial_2 \partial_2 H_2(\mathbf{x}^{(2)}) + \omega_2 I \end{bmatrix}, \quad (62)$$

583 where  $\partial_1 = \frac{\partial}{\partial \mathbf{x}^{(1)}}$  and  $\partial_2 = \frac{\partial}{\partial \mathbf{x}^{(2)}}$ . Like in the spherical spin  
584 glasses, fixing the trace of the Hessian to  $\mu$  is equivalent to  
585 a constraint on the Lagrange multipliers. However, in this  
586 case it corresponds to  $\mu = \omega_1 + \omega_2$ , and therefore they are  
587 not uniquely fixed by fixing  $\mu$ .

588 Since the energy in the multispherical models is Gaussian,  
589 the properties of the matrix  $\partial \partial H$  are again independent of the  
590 energy and gradient. This means that the form of the Hessian  
591 is parameterized solely by the values of the Lagrange multipliers

592  $\omega_1$  and  $\omega_2$ , just as  $\mu = \omega$  alone parameterized the Hessian  
593 in the spherical spin glasses. Unlike that case, however, the  
594 Hessian takes different shapes with different spectral widths  
595 depending on their precise combination. In Appendix C we  
596 derive a variational form for the spectral density of the Hessian  
597 in these models using standard methods.

598 Because of the independence of the Hessian, the method  
599 introduced in this article is not necessary to characterize the  
600 marginal minima of this system. Rather, we could take the  
601 spectral density derived in Appendix C and find the Lagrange  
602 multipliers  $\omega_1$  and  $\omega_2$  corresponding with marginality by tuning  
603 the edge of the spectrum to zero. In some ways the current  
604 method is more convenient than this, since it is a purely  
605 variational method and therefore can be reduced to a single  
606 root-finding exercise.

607 Unlike the constraints on the configurations  $\mathbf{x}$ , the constraint  
608 on the tangent vectors  $\mathbf{s} = [\mathbf{s}^{(1)}, \mathbf{s}^{(2)}] \in \mathbb{R}^{2N}$  remains  
609 the same spherical constraint as before, which implies  $N =$   
610  $\|\mathbf{s}\|^2 = \|\mathbf{s}^{(1)}\|^2 + \|\mathbf{s}^{(2)}\|^2$ . Defining intra- and inter-sphere  
611 overlap matrices

$$Q_{ab}^{ij,\alpha\gamma} = \frac{1}{N} \mathbf{s}_a^{(i),\alpha} \cdot \mathbf{s}_b^{(j),\gamma}, \quad (63)$$

612 this problem no longer has the property that the diagonal of  
613 the  $Q$ s is one, but instead that  $1 = Q_{aa}^{11,\alpha\alpha} + Q_{aa}^{22,\alpha\alpha}$ . This is  
614 the manifestation of the fact that a normalized vector in the  
615 tangent space of the multispherical model need not be equally  
616 spread over the two subspaces but can be concentrated in one  
617 or the other.

618 The calculation of the marginal complexity in this problem  
619 follows very closely to that of the spherical spin glasses in the  
620 previous subsection. We immediately make the simplifying  
621 assumptions that the soft directions of different stationary  
622 points are typically uncorrelated and therefore  $X = \hat{X} = 0$   
623 and the overlaps  $Q$  between eigenvectors are only nonzero  
624 when in the same replica. The result for the complexity has  
625 the schematic form of (51), but with different effective actions  
626 depending now on overlaps inside each of the two spheres  
627 and between the two spheres. The effective action for the  
628 traditional complexity of the multispherical spin glass is

$$\begin{aligned} & \mathcal{S}_{\text{MSG}}(\hat{\beta}, C^{11}, R^{11}, D^{11}, G^{11}, C^{22}, R^{22}, D^{22}, G^{22}, C^{12}, R^{12}, R^{21}, D^{12}, G^{12}, G^{21} | E, \omega_1, \omega_2) \\ &= \hat{\beta}(E - E_1 - E_2 - \epsilon c_d^{12}) + \mathcal{S}_{\text{SSG}}(\hat{\beta}, C^{11}, R^{11}, D^{11}, G^{11} | E_1, \omega_1) \\ &+ \mathcal{S}_{\text{SSG}}(\hat{\beta}, C^{22}, R^{22}, D^{22}, G^{22} | E_2, \omega_2) + \lim_{n \rightarrow 0} \frac{1}{n} \left\{ \epsilon \text{Tr}(R^{12} + R^{21} + G^{12} + G^{21} - \hat{\beta} C^{12}) \right. \\ &+ \left. \frac{1}{2} \log \det \left( I - \begin{bmatrix} C^{11} & iR^{11} \\ iR^{11} & D^{11} \end{bmatrix}^{-1} \begin{bmatrix} C^{12} & iR^{12} \\ iR^{21} & D^{12} \end{bmatrix} \begin{bmatrix} C^{22} & iR^{22} \\ iR^{22} & D^{22} \end{bmatrix}^{-1} \begin{bmatrix} C^{12} & iR^{21} \\ iR^{21} & D^{12} \end{bmatrix} \right) - \log \det(I - (G^{11} G^{22})^{-1} G^{12} G^{21}) \right\}, \end{aligned} \quad (64)$$

629 which is the sum of two effective actions (52) for the spherical spin glass associated with each individual sphere, and some  
630 coupling terms. The order parameters are defined the same as in the spherical spin glasses, but now with raised indices to  
631 indicate whether the vectors come from one or the other spherical subspace. The effective action for the eigenvalue-dependent

part of the complexity is likewise given by

$$\begin{aligned} \mathcal{U}_{\text{MSG}}(\hat{q}, \hat{\lambda}, Q^{11}, Q^{22}, Q^{12} | \beta, \lambda^*, \omega_1, \omega_2) \\ = \lim_{m \rightarrow 0} \left\{ \sum_{\alpha=1}^m [\hat{q}^\alpha (Q^{11, \alpha\alpha} + Q^{22, \alpha\alpha} - 1) - \beta(\omega_1 Q^{11, \alpha\alpha} + \omega_2 Q^{22, \alpha\alpha} - 2\epsilon Q^{12, \alpha\alpha})] - \hat{\lambda}(\omega_1 Q^{11, 11} + \omega_2 Q^{22, 11} - 2\epsilon Q^{12, 11}) \right. \\ \left. + \sum_{i=1,2} f_i''(1) \left[ \beta^2 \sum_{\alpha\gamma} (Q^{ii, \alpha\gamma})^2 + 2\beta\hat{\lambda} \sum_{\alpha} (Q^{ii, 1\alpha})^2 + \hat{\lambda}^2 (Q^{ii, 11})^2 \right] + \frac{1}{2} \log \det \begin{bmatrix} Q^{11} & Q^{12} \\ Q^{12} & Q^{22} \end{bmatrix} \right\}. \end{aligned} \quad (65)$$

The new variables  $\hat{q}^\alpha$  are Lagrange multipliers introduced to enforce the constraint that  $Q^{11, \alpha\alpha} + Q^{22, \alpha\alpha} = 1$ . Because of this constraint, the diagonal of the  $Q$  matrices cannot be taken to be one as in Sec. II B. Instead we take each of the matrices  $Q^{11}$ ,  $Q^{22}$ , and  $Q^{12}$  to have the planted replica symmetric form of (9), but with the diagonal not necessarily equal to one, so

$$Q^{ij} = \begin{bmatrix} \tilde{q}_d^{ij} & \tilde{q}_0^{ij} & \tilde{q}_0^{ij} & \cdots & \tilde{q}_0^{ij} \\ \tilde{q}_0^{ij} & q_d^{ij} & q_0^{ij} & \cdots & q_0^{ij} \\ \tilde{q}_0^{ij} & q_0^{ij} & q_d^{ij} & \cdots & q_0^{ij} \\ \vdots & \vdots & \cdots & \ddots & \vdots \\ \tilde{q}_0^{ij} & q_0^{ij} & q_0^{ij} & \cdots & q_d^{ij} \end{bmatrix}. \quad (66)$$

This requires us to introduce two new order parameters  $\tilde{q}_d^{ij}$  and  $q_d^{ij}$  per pair  $(i, j)$ , in addition to the off-diagonal order parameters  $\tilde{q}_0^{ij}$  and  $q_0^{ij}$  already present in (9). We also need two separate Lagrange multipliers  $\hat{q}$  and  $\hat{\tilde{q}}$  to enforce the tangent space normalization  $q_d^{11} + q_d^{22} = 1$  and  $\tilde{q}_d^{11} + \tilde{q}_d^{22} = 1$  for the tilde and untilde replicas, respectively, which will in general take different values at the saddle point. When this ansatz is inserted into the expression (65) for the effective action and the limit of  $m \rightarrow 0$  is taken, we find

$$\begin{aligned} \mathcal{U}_{\text{MSG}}(\hat{q}, \hat{\tilde{q}}, \hat{\lambda}, \tilde{q}_d^{11}, \tilde{q}_0^{11}, q_d^{11}, q_0^{11}, \tilde{q}_d^{22}, \tilde{q}_0^{22}, q_d^{22}, q_0^{22}, \tilde{q}_d^{12}, \tilde{q}_0^{12}, q_d^{12}, q_0^{12} | \beta, \lambda^*, \omega_1, \omega_2) \\ = \sum_{i=1,2} \{ f_i''(1) [\beta^2 ((\tilde{q}_d^{ii})^2 - (q_d^{ii})^2) + 2(q_0^{ii})^2 - 2(\tilde{q}_0^{ii})^2] + 2\beta\hat{\lambda} ((\tilde{q}_d^{ii})^2 - (q_0^{ii})^2) + \hat{\lambda}^2 (\tilde{q}_d^{ii})^2 \} - \hat{\lambda} \tilde{q}_d^{ii} \omega_i - \beta (\tilde{q}_d^{ii} - q_d^{ii}) \omega_i \\ + \frac{1}{2} \log [(2q_0^{12} \tilde{q}_0^{12} - \tilde{q}_0^{12} (\tilde{q}_d^{12} + q_d^{12}) - 2\tilde{q}_0^{11} q_0^{22} + \tilde{q}_d^{11} \tilde{q}_0^{22} + \tilde{q}_0^{11} q_d^{22}) (2q_0^{12} \tilde{q}_0^{12} - \tilde{q}_0^{12} (\tilde{q}_d^{12} + q_d^{12}) - 2q_0^{11} \tilde{q}_0^{22} + q_d^{11} \tilde{q}_0^{22} \\ + \tilde{q}_0^{11} \tilde{q}_d^{22}) + 2(3(q_0^{12})^2 - (\tilde{q}_0^{12})^2 - 2q_0^{12} q_d^{12} - 3q_0^{11} q_0^{22} + q_d^{11} q_0^{22} + \tilde{q}_0^{11} \tilde{q}_d^{22} + q_0^{11} q_d^{22}) ((\tilde{q}_d^{12})^2 - (\tilde{q}_d^{12})^2 - \tilde{q}_0^{11} \tilde{q}_d^{22} + \tilde{q}_d^{11} \tilde{q}_d^{22}) \\ - (2(q_0^{12})^2 - (\tilde{q}_0^{12})^2 - (q_d^{12})^2 - 2q_0^{11} q_0^{22} + \tilde{q}_0^{11} \tilde{q}_d^{22} + q_d^{11} q_d^{22}) ((\tilde{q}_d^{12})^2 - (\tilde{q}_d^{12})^2 - \tilde{q}_0^{11} \tilde{q}_d^{22} + \tilde{q}_d^{11} \tilde{q}_d^{22})] \\ - \log [(q_d^{11} - q_0^{11})(q_d^{22} - q_0^{22}) - (q_d^{12} - q_0^{12})^2] + 2\epsilon [\hat{\lambda} \tilde{q}_d^{12} + \beta (\tilde{q}_d^{12} - q_d^{12})] - \hat{q} (q_d^{11} + q_d^{22} - 1) + \hat{\tilde{q}} (\tilde{q}_d^{11} + \tilde{q}_d^{22} - 1). \end{aligned} \quad (67)$$

To make the limit to zero temperature, we once again need an ansatz for the asymptotic behavior of the overlaps. These take the form  $q_0^{ij} = q_d^{ij} - y_0^{ij} \beta^{-1} - z_0^{ij} \beta^{-2}$ . Notice that in this case, the asymptotic behavior of the off-diagonal elements is to approach the value of the diagonal rather than to approach one. We also require  $\tilde{q}_d^{ij} = q_d^{ij} - \tilde{y}_d^{ij} \beta^{-1} - \tilde{z}_d^{ij} \beta^{-2}$ , i.e., that the tilde diagonal terms also approach the same diagonal value as the untilde terms, but with potentially different rates.

As before, in order for the logarithmic term to stay finite, there are necessary constraints on the values  $y$ . These are

$$\frac{1}{2} (y_d^{11} - \tilde{y}_d^{11}) = y_0^{11} - \tilde{y}_0^{11}, \quad (68)$$

$$\frac{1}{2} (y_d^{22} - \tilde{y}_d^{22}) = y_0^{22} - \tilde{y}_0^{22}, \quad (69)$$

$$\frac{1}{2} (y_d^{12} - \tilde{y}_d^{12}) = y_0^{12} - \tilde{y}_0^{12}. \quad (70)$$

One can see that when the diagonal elements are all equal, this requires the  $y$ s for the off-diagonal elements to be equal, as in the GOE case. Here, since the diagonal elements are not necessarily equal, we have a more general relationship.

When the  $\beta$  dependence of the  $q$  variables is inserted into the effective action (67) and the limit  $\beta \rightarrow \infty$  taken, we find an expression that is too large to report here. However, it can be extremized over all of the variables in the problem just as in the previous examples to find the values of the Lagrange multipliers  $\omega_1$  and  $\omega_2$  corresponding to marginal minima. Figure 2(a) shows examples of the  $\omega_1$  and  $\omega_2$  corresponding to marginal spectra for a variety of couplings  $\epsilon$  when the covariances of the energy on the two spherical subspaces are such that  $1 = f_1''(1) = f_2''(1)$ . Figure 2(b) shows the Hessian spectra associated with some specific pairs  $(\omega_1, \omega_2)$ . When  $\epsilon = 0$  and the two spheres are uncoupled, we find the result for two independent spherical spin glasses: if either  $\omega_1 = 2\sqrt{f''(1)} =$

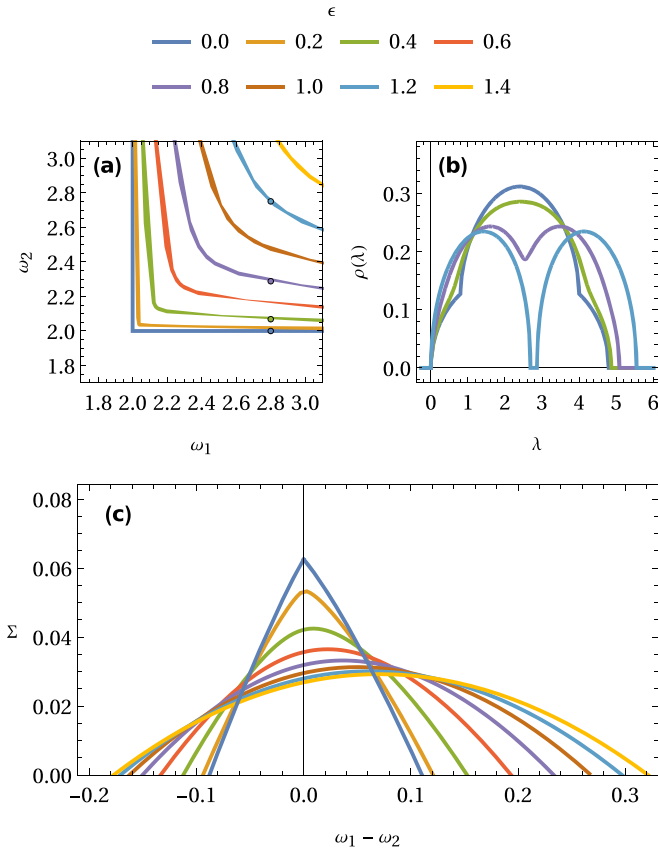


FIG. 2. Properties of marginal minima in the multispherical model. (a) Values of the Lagrange multipliers  $\omega_1$  and  $\omega_2$  corresponding to a marginal spectrum for multispherical spin glasses with  $\sigma_1^2 = f_1''(1) = 1$ ,  $\sigma_2^2 = f_2''(1) = 1$ , and various  $\epsilon$ . (b) Spectra corresponding to the parameters  $\omega_1$  and  $\omega_2$  marked by the circles in panel (a). (c) The complexity of marginal minima in a multispherical model with  $f_1(q) = \frac{1}{6}q^3$  and  $f_2(q) = \frac{1}{12}q^4$  for a variety of  $\epsilon$ . Since  $f_1''(1) = f_2''(1) = 1$ , the marginal values correspond precisely to those in panels (a) and (b).

2 or  $\omega_2 = 2\sqrt{f''(1)} = 2$  and the other Lagrange multiplier is larger than two, then we have a marginal minimum made up of the Cartesian product of a marginal minimum on one subspace and a stable minimum on the other.

Fig. 2(c) shows the complexity of marginal minima in an example where both  $H_1$  and  $H_2$  correspond to pure  $p$ -spin models, with  $f_1(q) = \frac{1}{6}q^3$  and  $f_2(q) = \frac{1}{12}q^4$ . Despite having different covariance functions, these both satisfy  $1 = f_1''(1) = f_2''(1)$  and therefore have marginal minima for Lagrange multipliers that satisfy the relationships in Fig. 2(a). In the uncoupled system with  $\epsilon = 0$ , the most common type of marginal stationary point consists of independently marginal stationary points in the two subsystems, with  $\omega_1 = \omega_2 = 2$ . As  $\epsilon$  is increased, the most common type of marginal minimum drifts toward points with  $\omega_1 > \omega_2$ .

Multispherical spin glasses may be an interesting platform for testing ideas about which among the possible marginal minima can attract dynamics and which cannot. In the limit where  $\epsilon = 0$  and the configurations of the two spheres are independent, the minima found dynamically should be marginal on both subspaces. Just because technically on the expanded

configuration space the Cartesian product of a deep stable minimum on one sphere and a marginal minimum on the other is a marginal minimum on the whole space doesn't mean the deep and stable minimum is any easier to find. This intuitive idea that is precise in the zero-coupling limit should continue to hold at small nonzero coupling, and perhaps reveal something about the inherent properties of marginal minima that do not tend to be found by algorithms.

### C. Sums of squared random functions

In this subsection we consider perhaps the simplest example of a non-Gaussian landscape: the problem of sums of squared random functions. This problem has a close resemblance to nonlinear least squares optimization. Though, for reasons we will see it is easier to make predictions for nonlinear *most* squares, i.e., the problem of maximizing the sum of squared terms. We again take a spherical configuration space with  $\mathbf{x} \in S^{N-1}$  and  $0 = g(\mathbf{x}) = \frac{1}{2}(\|\mathbf{x}\|^2 - N)$  as in the spherical spin glasses. The energy is built from a set of  $M = \alpha N$  random functions  $V_k : S^{N-1} \rightarrow \mathbb{R}$  that are centered Gaussians with covariance

$$\overline{V_i(\mathbf{x})V_j(\mathbf{x}')} = \delta_{ij}f\left(\frac{\mathbf{x} \cdot \mathbf{x}'}{N}\right). \quad (71)$$

Each of the  $V_k$  is an independent spherical spin glass. The total energy is minus the sum of squares of the  $V_k$ , or

$$H(\mathbf{x}) = -\frac{1}{2} \sum_{k=1}^M V_k(\mathbf{x})^2. \quad (72)$$

The landscape complexity and large deviations of the ground state for the least-squares version of this problem were recently studied in a linear context, with  $f(q) = \sigma^2 + \alpha q$  [42–45]. Some results on the ground state of the general nonlinear problem can also be found in Ref. [46], and a solution to the equilibrium problem can be found in Ref. [47]. Those works indicate that the low-lying minima of the least squares problem tend to be either replica symmetric or full replica symmetry breaking. To avoid either a trivial analysis or a very complex one, we instead focus on maximizing the sum of squares, or minimizing (72).

The minima of (72) have a more amenable structure for study than the maxima, as they are typically described by a 1RSB-like structure. There is a heuristic intuition for this: in the limit of  $M \rightarrow 1$ , this problem is just minus the square of a spherical spin glass landscape. The distribution and properties of stationary points low and high in the spherical spin glass are not changed, except that their energies are stretched and maxima are transformed into minima. Therefore, the bottom of the landscape doesn't qualitatively change. The top, however, consists of the zero-energy level set in the spherical spin glass. This level set is well connected, and so the highest states should also be well connected and flat.

Focusing on the bottom of the landscape and therefore dealing with a 1RSB-like problem makes our analysis easier. Algorithms will tend to be stuck in the ways they are in hard optimization problems, and we will be able to predict where.

738 Therefore, we will study the most squares problem rather  
 739 than the least squares one. We calculate the complexity of  
 740 minima of (72) in Appendix D, which corresponds to maxi-  
 741 mizing the sum of squares, under a replica symmetric ansatz  
 742 (which covers IRSB-like problems) for arbitrary covariance  $f$ ,  
 743 and we calculate the complexity of marginal minima in this  
 744 section.

745 As in the previous sections, we used the method of  
 746 Lagrange multipliers to analyze stationary points on the  
 747 constrained configuration space. The Lagrangian and its as-  
 748 sociated gradient and Hessian are

$$L(\mathbf{x}, \omega) = -\frac{1}{2} \left( \sum_k^M V_k(\mathbf{x})^2 - \omega(\|\mathbf{x}\|^2 - N) \right), \quad (73)$$

$$\nabla H(\mathbf{x}, \omega) = - \sum_k^M V_k(\mathbf{x}) \partial V_k(\mathbf{x}) + \omega \mathbf{x}, \quad (74)$$

$$\text{Hess } H(\mathbf{x}, \omega) = - \sum_k^M [\partial V_k(\mathbf{x}) \partial V_k(\mathbf{x}) - V_k(\mathbf{x}) \partial \partial V_k(\mathbf{x})] + \omega I. \quad (75)$$

749 Unlike in the spherical and multispherical spin glasses, the  
 750 value  $\mu^*$  defined in (38) giving the typical value of  $\frac{1}{N} \text{Tr } \partial \partial H$   
 751 is not always zero. Instead  $\mu^* = -f'(0)$ , nonzero where there  
 752 is a linear term in  $V$ . Fixing the trace of the Hessian is  
 753 therefore equivalent to constraining the value of the Lagrange  
 754 multiplier  $\omega = \mu + f'(0)$ .

755 The derivation of the marginal complexity for this model  
 756 is complicated, but can be made schematically like that of the  
 757 derivation of the equilibrium free energy by use of superspace  
 758 coordinates. Following the framework outlined in Sec. III C,  
 759 the replicated number of stationary points conditioned on  
 760 energy  $E$ , trace  $\mu$ , and minimum eigenvalue  $\lambda^*$  is given by

$$\mathcal{N}(E, \mu, \lambda^*)^n = \int d\hat{\beta} d\hat{\lambda} \prod_{a=1}^n \lim_{m_a \rightarrow 0} \prod_{\alpha=1}^{m_a} d\phi_a^\alpha \times \exp \left\{ \delta^{\alpha 1} N(\hat{\beta} E + \hat{\lambda} \lambda^*) - \frac{1}{2} \int d1 d2 \left[ B^\alpha(1, 2) \sum_{k=1}^M V_k(\phi_a^\alpha(1, 2))^2 - (\mu + f'(0)) \|\phi_a^\alpha(1, 2)\|^2 \right] \right\}, \quad (76)$$

The first step to evaluate this expression is to linearize the dependence on the random functions  $V$ . This is accomplished by inserting into the integral a Dirac  $\delta$  function fixing the value of the energy for each replica, or

$$\delta(V_k(\phi_a^\alpha(1, 2)) - v_{ka}^\alpha(1, 2)) = \int d\hat{v}_{ka}^\alpha \exp \left[ i \int d1 d2 \hat{v}_{ka}^\alpha(1, 2) (V_k(\phi_a^\alpha(1, 2)) - v_{ka}^\alpha(1, 2)) \right], \quad (77)$$

763 where we have introduced auxiliary superfields  $\hat{v}$ . With this inserted into the integral, all other instances of  $V$  are replaced by  $v$ ,  
 764 and the only remaining dependence on the disorder is from the term  $\hat{v}V$  arising from the Fourier representation of the Dirac  $\delta$   
 765 function. This term is linear in  $V$ , and therefore the random functions can be averaged over to produce

$$\overline{\exp \left[ i \sum_k^M \sum_a^n \sum_\alpha^{m_a} \int d1 d2 \hat{v}_{ka}^\alpha(1, 2) V_k(\phi_a^\alpha(1, 2)) \right]} = -\frac{1}{2} \sum_{ab}^n \sum_{\alpha\gamma}^{m_a} \sum_k^M \int d1 d2 d3 d4 \hat{v}_{ka}^\alpha(1, 2) f(\phi_a^\alpha(1, 2) \cdot \phi_b^\gamma(3, 4)) \hat{v}_{kb}^\gamma(3, 4). \quad (78)$$

766 The entire integrand is now factorized in the indices  $k$  and quadratic in the superfields  $v$  and  $\hat{v}$  with the kernel

$$\begin{bmatrix} B^\alpha(1, 2) \delta(1, 3) \delta(2, 4) \delta_{ab} \delta^{\alpha\gamma} & i \delta(1, 3) \delta(2, 4) \delta_{ab} \delta^{\alpha\gamma} \\ i \delta(1, 3) \delta(2, 4) \delta_{ab} \delta^{\alpha\gamma} & f(\phi_a^\alpha(1, 2) \cdot \phi_b^\gamma(3, 4)) \end{bmatrix}. \quad (79)$$

767 The integration over  $v$  and  $\hat{v}$  results in a term in the effective action of the form

$$-\frac{M}{2} \log \text{sdet} \left[ \delta(1, 3) \delta(2, 4) \delta_{ab} \delta^{\alpha\gamma} + B^\alpha(1, 2) f(\phi_a^\alpha(1, 2) \cdot \phi_b^\gamma(3, 4)) \right]. \quad (80)$$

768 When expanded, the supermatrix  $\phi_a^\alpha(1, 2) \cdot \phi_b^\gamma(3, 4)$  is constructed of the scalar products of the real and Grassmann vectors that  
 769 make up  $\phi$ . The change of variables to these order parameters again results in the Jacobian of (50), contributing

$$\frac{N}{2} \log \det J - \frac{N}{2} \log \det G^2 \quad (81)$$

770 to the effective action.

771 Up to this point, the expressions are general and independent of a given ansatz. However, we expect that the order parameters  
 772  $X$  and  $\hat{X}$  are zero, since again we are in a setting with no signal or external field. Applying this ansatz here avoids a dramatically  
 773 more complicated expression for the effective action. We also will apply the ansatz that  $Q_{ab}^{\alpha\gamma}$  is zero for  $a \neq b$ , which is  
 774 equivalent to assuming that the soft directions of typical pairs of stationary points are uncorrelated, and further that  $Q^{\alpha\gamma} = Q_{aa}^{\alpha\gamma}$   
 775 independently of the index  $a$ , implying that correlations in the tangent space of typical stationary points are the same.

776 Given this ansatz, taking the superdeterminant in (80) yields

$$\begin{aligned}
 & -\frac{M}{2} \log \det \left\{ \left[ f'(C) \odot D - \hat{\beta}I + \left( R^{\circ 2} - G^{\circ 2} + I \sum_{\alpha\gamma} 2(\delta^{\alpha 1} \hat{\lambda} + \beta)(\delta^{\gamma 1} \hat{\lambda} + \beta)(Q^{\alpha\gamma})^2 \right) \odot f''(C) \right] f(C) + (I - R \odot f'(C))^2 \right\} \\
 & - n \frac{M}{2} \log \det[\delta_{\alpha\gamma} - 2(\delta_{\alpha 1} \hat{\lambda} + \beta)Q^{\alpha\gamma}] + M \log \det[I + G \odot f'(C)]. \tag{82}
 \end{aligned}$$

777 where once again  $\odot$  is the Hadamard product and  $A^{\circ n}$  gives the Hadamard power of  $A$ . We can already see one substantive  
 778 difference between the structure of this problem and that of the spherical models: the effective action in this case mixes the  
 779 order parameters  $G$  due to the Grassmann variables with the ones  $C$ ,  $R$ , and  $D$  due to the other variables. Notice further that the  
 780 dependence on  $Q$  due to the marginal constraint is likewise no longer separable into its own term. This is the realization of the  
 781 fact that the Hessian is no longer independent of the energy and gradient.

782 Now we have reduced the problem to an extremal one over the order parameters  $\hat{\beta}$ ,  $\hat{\lambda}$ ,  $C$ ,  $R$ ,  $D$ ,  $G$ , and  $Q$ , it is time to make  
 783 an ansatz for the form of order we expect to find. We will focus on a regime where the structure of stationary points is replica  
 784 symmetric, and further where typical pairs of stationary points have no overlap. This requires that  $f(0) = 0$ , or that there is no  
 785 constant term in the random functions. This gives the ansatz

$$C = I, \quad R = rI, \quad D = dI, \quad G = gI. \tag{83}$$

786 We further take a planted replica symmetric structure for the matrix  $Q$ , identical to that in (9). This results in

$$\Sigma_{\lambda^*}(E, \mu) = \frac{1}{N} \lim_{n \rightarrow 0} \frac{\partial}{\partial n} \int d\hat{\beta} d\hat{\lambda} dr dd dg dq_0 d\tilde{q}_0 e^{nN \mathcal{S}_{\text{RSS}}(\hat{\beta}, \hat{\lambda}, r, d, g, q_0, \tilde{q}_0 | \lambda^*, E, \mu, \beta)}, \tag{84}$$

787 with an effective action

$$\begin{aligned}
 & \mathcal{S}_{\text{RSS}}(\hat{\beta}, \hat{\lambda}, r, d, g, q_0, \tilde{q}_0 | \lambda^*, E, \mu, \beta) \\
 & = \hat{\beta}E - (\mu + f'(0))(r + g + \hat{\lambda}) + \hat{\lambda}\lambda^* + \frac{1}{2} \log \left( \frac{d + r^2}{g^2} \times \frac{1 - 2q_0 + \tilde{q}_0^2}{(1 - q_0)^2} \right) \\
 & - \frac{\alpha}{2} \log \left( \frac{1 - 4f'(1)[\beta(1 - q_0) + \frac{1}{2}\hat{\lambda} - \beta(\beta + \hat{\lambda})(1 - 2q_0 + \tilde{q}_0^2)]f'(1)}{[1 - 2(1 - q_0)\beta f'(1)]^2} \right) \\
 & \times \frac{f(1)[f'(1)d - \hat{\beta} - f''(1)(r^2 - g^2 + 4q_0^2\beta^2 - 4\tilde{q}_0^2\beta(\beta + \hat{\lambda}) + 4\beta\hat{\lambda} + 2\hat{\lambda}^2)] + (1 - rf'(1))^2}{[1 + gf'(1)]^2}. \tag{85}
 \end{aligned}$$

788 We expect as before the limits of  $q_0$  and  $\tilde{q}_0$  as  $\beta$  goes to infinity to approach one, defining their asymptotic expansion like in (15)  
 789 and (16). Upon making this substitution and taking the zero-temperature limit, we find

$$\begin{aligned}
 \mathcal{S}_{\text{RSS}}(\hat{\beta}, \hat{\lambda}, r, d, g, y, \Delta z | \lambda^*, E, \mu, \infty) & = \hat{\beta}E - (\mu + f'(0))(r + g + \hat{\lambda}) + \hat{\lambda}\lambda^* + \frac{1}{2} \log \left( \frac{d + r^2}{g^2} \times \frac{y^2 - 2\Delta z}{y^2} \right) \\
 & - \frac{\alpha}{2} \log \left( \frac{1 - 2(2y + \hat{\lambda})f'(1) + 4(y^2 - 2\Delta z)f'(1)^2}{[1 - 2yf'(1)]^2} \right) \\
 & \times \frac{f(1)[f'(1)d - \hat{\beta} - f''(1)(r^2 - g^2 + 8(y\hat{\lambda} + \Delta z) + 2\hat{\lambda}^2)] + [1 - rf'(1)]^2}{[1 + gf'(1)]^2}. \tag{86}
 \end{aligned}$$

790 We can finally write the complexity with fixed energy  $E$ ,  
 791 stability  $\mu$ , and minimum eigenvalue  $\lambda^*$  as

$$\begin{aligned}
 \Sigma_{\lambda^*}(E, \mu) & = \text{extremum}_{\hat{\beta}, \hat{\lambda}, r, d, g, y, \Delta z} \mathcal{S}_{\text{RSS}}(\hat{\beta}, \hat{\lambda}, r, d, g, y, \Delta z | \lambda^*, E, \mu, \infty). \tag{87}
 \end{aligned}$$

792 Note that, unlike the previous two examples, the effective  
 793 action in this case does not split into two largely independent  
 794 pieces, one relating to the eigenvalue problem and one relating  
 795 to the ordinary complexity. Instead, the order parameters  
 796 related to the eigenvalue problem are mixed throughout the  
 797 effective action with those of the ordinary complexity. This

798 is a signal of the fact that the sum of squares problem is not  
 799 Gaussian, while the previous two examples are. In all non-  
 800 Gaussian problems, conditioning on properties of the Hessian  
 801 cannot be done independently from the complexity, and the  
 802 method introduced in this paper becomes necessary.

803 The marginal complexity can be derived from (87) using  
 804 the condition (32) to fix  $\mu$  to the marginal stability  $\mu_m(E)$   
 805 and then evaluating the complexity at that stability as in (33).  
 806 Figure 3 shows the marginal complexity in a sum-of-squares  
 807 model with  $\alpha = \frac{3}{2}$  and  $f(q) = q^2 + q^3$ . Also shown is the  
 808 dominant complexity computed in Appendix D. As the figure  
 809 demonstrates, the range of energies at which marginal minima  
 810 are found can differ significantly from those implied by the  
 811 dominant complexity, with the lowest energy significantly

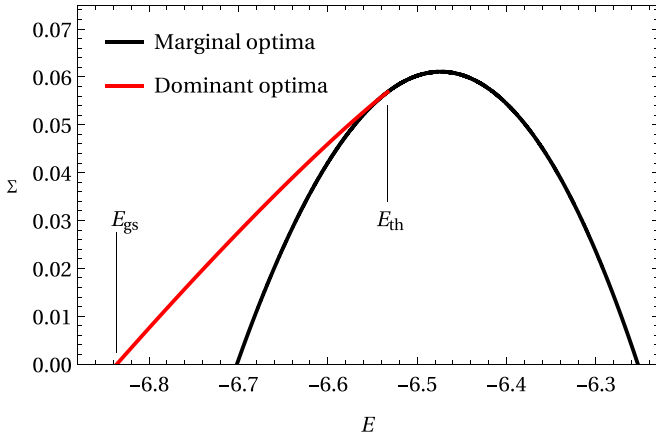


FIG. 3. Dominant and marginal complexity in the nonlinear sum of squares problem for  $\alpha = \frac{3}{2}$  and  $f(q) = q^2 + q^3$ . The ground-state energy  $E_{\text{gs}}$  and the threshold energy  $E_{\text{th}}$  are marked on the plot.

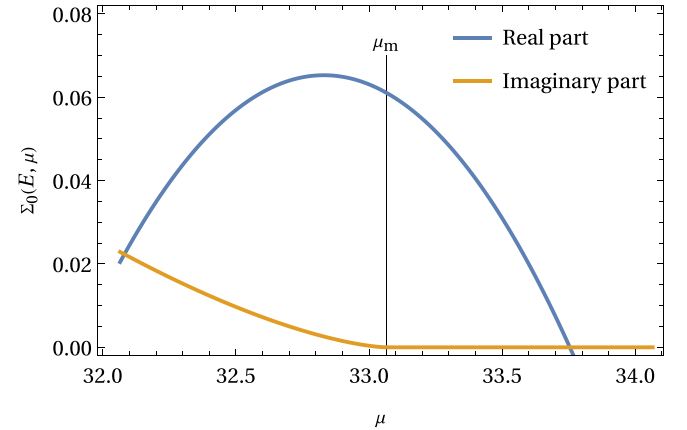


FIG. 5. Real and imaginary parts of the complexity  $\Sigma_0(E, \mu)$  with fixed minimum eigenvalue  $\lambda^* = 0$  as a function of  $\mu$  in the nonlinear sum of squares problem with  $\alpha = \frac{3}{2}$ ,  $f(q) = q^2 + q^3$ , and  $E \simeq -6.47$ . The vertical line depicts the value of the marginal stability  $\mu_m$ .

812 higher than the ground state and the highest energy significantly  
813 higher than the threshold.

814 Figure 4 shows the associated marginal stability  $\mu_m(E)$  for  
815 the same model. Recall that the definition of the marginal  
816 stability in (32) is that which eliminates the variation of  
817  $\Sigma_{\lambda^*}(E, \mu)$  with respect to  $\lambda^*$  at the point  $\lambda^* = 0$ . Unlike in the  
818 Gaussian spherical spin glass, in this model  $\mu_m(E)$  varies with  
819 energy in a nontrivial way. The figure also shows the dominant  
820 stability, which is the stability associated with the dominant  
821 complexity and coincides with the marginal stability only at  
822 the threshold energy.

823 Because this version of the model has no signal, we were  
824 able to use the heuristic (32) to fix the marginal stability.  
825 However, we could also have used the more general method  
826 for finding a pseudogapped Hessian spectrum by locating the  
827 value of  $\mu$  at which the complexity develops an imaginary  
828 part, as described in Sec. II C and pictured in Fig. 1. The real  
829 and imaginary parts of the complexity  $\Sigma_0(E, \mu)$  are plotted  
830 in Fig. 5 as a function of  $\mu$  at fixed energy. The figure also  
831 shows the marginal stability  $\mu_m$  predicted by the variational

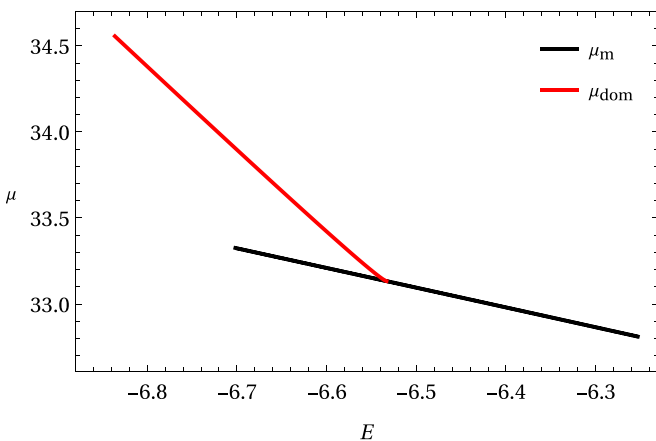


FIG. 4. The stability, or shift of the trace, for dominant and marginal optima in the nonlinear sum of squares problem for  $\alpha = \frac{3}{2}$  and  $f(q) = q^2 + q^3$ .

832 approach (32). The marginal stability corresponds to precisely  
833 the point at which an imaginary part develops in the complex-  
834 ity. This demonstrates that the principles we used to determine  
835 the marginal stability continue to hold even in non-Gaussian  
836 cases where the complexity and the condition to fix the mini-  
837 mum eigenvalue are tangled together.

838 In a related paper, we use a sum of squared random func-  
839 tions model to explore the relationship between the marginal  
840 complexity and the performance of two generic algorithms:  
841 gradient descent and approximate message passing [21]. We  
842 show that the range of energies where the marginal complexity  
843 is positive does effectively bound the performance of these  
844 algorithms. At the moment the comparison is restricted to  
845 models with small polynomial powers appearing in  $f(q)$  and  
846 with small  $\alpha$  for computational reasons. However, using the  
847 dynamical mean-field theory results already found for these  
848 models it should be possible to make comparisons in a wider  
849 family of models [48,49].

850 The results for the marginal complexity are complimentary  
851 to rigorous results on the performance of algorithms in the  
852 least squares case, which focus on bounds for  $\alpha$  and the  
853 parameters of  $f$  necessary for zero-energy solutions to exist  
854 and be found by algorithms [50,51]. After more work to eval-  
855 uate the marginal complexity in the full RSB case, it will be  
856 interesting to compare the bounds implied by the distribution  
857 of marginal minima with those made by other means.

## V. CONCLUSIONS

858 We have introduced a method for conditioning complex-  
859 ity on the marginality of stationary points. This method is  
860 general, and permits conditioning without first needing to  
861 understand the statistics of the Hessian at stationary points.  
862 We used our approach to study marginal complexity in three  
863 different models of random landscapes, showing that the  
864 method works and can be applied to models whose marginal  
865 complexity was not previously known. In related work, we  
866 further show that marginal complexity in the third model of  
867

868 sums of squared random functions can be used to effectively  
869 bound algorithmic performance [21].

870 There are some limitations to the approach we relied on in  
871 this paper. The main limitation is our restriction to signalless  
872 landscapes, where there is no symmetry-breaking favored di-  
873 rection. This allowed us to treat stationary points with isolated  
874 eigenvalues as atypical and therefore find the marginal stabil-  
875 ity  $\mu_m$  using a variational principle. However, most models  
876 of interest in inference have a nonzero signal strength and  
877 therefore often have typical stationary points with an isolated  
878 eigenvalue. As we described, marginal complexity can still  
879 be analyzed in these systems by tuning the shift  $\mu$  until the  
880 large-deviation principle breaks down and an imaginary part  
881 of the complexity appears. However, this is an inconvenient  
882 approach. It is possible that a variational approach can be  
883 preserved by treating the direction toward and the directions  
884 orthogonal to the signal differently. This problem merits fur-  
885 ther research.

886 Finally, the problem of predicting which marginal minima  
887 are able to attract some dynamics and which cannot attract  
888 any dynamics looms large over this work. As we discussed  
889 briefly at the end of Sec. IV B, in some simple contexts it is  
890 easy to see why certain marginal minima are not viable, but  
891 at the moment we do not know how to generalize this. Ideas  
892 related to the self-similarity and stochastic stability of minima  
893 have recently been suggested as a route to understanding this  
894 problem, but this approach is still in its infancy [52].

895 The title of our paper and that of Müller *et al.* suggest  
896 they address the same topic, but this is not the case [53]. That  
897 work differs in three important and fundamental ways. First,  
898 it describes minima of the Thouless, Anderson, and Palmer  
899 (TAP) free energy and involves peculiarities specific to the  
900 TAP. Second, it describes dominant minima which happen to  
901 be marginal, not a condition for finding subdominant marginal  
902 minima. Finally, it focuses on minima with a single soft di-  
903 rection (which are the typical minima of the low temperature  
904 Sherrington–Kirkpatrick TAP free energy), while we aim to  
905 avoid such minima in favor of ones that have a pseudogap  
906 (which we argue are relevant to out-of-equilibrium dynamics).  
907 The fact that the typical minima studied by Müller *et al.*  
908 are not marginal in this latter sense may provide an intuitive  
909 explanation for the seeming discrepancy between the proof  
910 that the low-energy Sherrington–Kirkpatrick model cannot be  
911 sampled [54] and the proof that a message-passing algorithm  
912 can find near-ground states [55]: the algorithm finds the atyp-  
913 ical low-lying states that are marginal in the sense considered  
914 here but cannot find the typical ones considered by Müller  
915 *et al.*

#### 916 ACKNOWLEDGMENTS

917 J.K.-D. was supported by a DYNYSMATH Specific Initia-  
918 tive of the INFN.

#### 919 APPENDIX A: A PRIMER ON SUPERSPACE

920 In this appendix we review the algebra of superspace [56].  
921 The superspace  $\mathbb{R}^{N|2D}$  is a vector space with  $N$  real indices and  
922  $2D$  Grassmann indices  $\bar{\theta}_1, \theta_1, \dots, \bar{\theta}_D, \theta_D$ . The Grassmann in-  
923 dices anticommute like fermions. Their integration is defined

by

$$\int d\theta \theta = 1, \quad \int d\theta 1 = 0. \quad (A1)$$

924 Because the Grassmann indices anticommute, their square is  
925 always zero. Therefore, any series expansion of a function  
926 with respect to a given Grassmann index will terminate ex-  
927 actly at linear order, while a series expansion with respect to  
928  $n$  Grassmann variables will terminate exactly at  $n$ th order. If  
929  $f$  is an arbitrary superspace function, then the integral of  $f$   
930 with respect to a Grassmann index can be evaluated using this  
931 property of the series expansion by  
932

$$\int d\theta f(a + b\theta) = \int d\theta [f(a) + f'(a)b\theta] = f'(a)b. \quad (A2)$$

933 This kind of behavior of integrals over the Grassmann indices  
934 makes them useful for compactly expressing the Kac–Rice  
935 measure. To see why, consider the specific superspace  $\mathbb{R}^{N|2}$ ,  
936 where an arbitrary vector can be expressed as

$$\phi(1) = \mathbf{x} + \bar{\theta}_1 \eta + \bar{\eta} \theta_1 + \bar{\theta}_1 \theta_1 i\hat{\mathbf{x}}, \quad (A3)$$

937 where  $\mathbf{x}, \hat{\mathbf{x}} \in \mathbb{R}^N$  and  $\bar{\eta}, \eta$  are  $N$ -dimensional Grassmann  
938 vectors. The dependence of  $\phi$  on 1 indicates the index of  
939 Grassmann variables  $\bar{\theta}_1, \theta_1$  inside, since we will sometimes  
940 want to use, e.g.,  $\phi(2)$  defined identically save for substitu-  
941 tion by  $\bar{\theta}_2, \theta_2$ . Consider the series expansion of an arbitrary  
942 function  $f$  of this supervector:

$$\begin{aligned} f(\phi(1)) &= f(\mathbf{x}) + (\bar{\theta}_1 \eta + \bar{\eta} \theta_1 + \bar{\theta}_1 \theta_1 i\hat{\mathbf{x}})^T \partial f(\mathbf{x}) \\ &\quad + \frac{1}{2} (\bar{\theta}_1 \eta + \bar{\eta} \theta_1)^T \partial \partial f(\mathbf{x}) (\bar{\theta}_1 \eta + \bar{\eta} \theta_1) \\ &= f(\mathbf{x}) + (\bar{\theta}_1 \eta + \bar{\eta} \theta_1 + \bar{\theta}_1 \theta_1 i\hat{\mathbf{x}})^T \partial f(\mathbf{x}) \\ &\quad - \bar{\theta}_1 \theta_1 \bar{\eta}^T \partial \partial f(\mathbf{x}) \eta, \end{aligned} \quad (A4)$$

943 where the last step we used the fact that the Hessian matrix  
944 is symmetric and that squares of Grassmann indices vanish.  
945 Using the integration rules defined above, we find

$$\int d\theta_1 d\bar{\theta}_1 f(\phi(1)) = i\hat{\mathbf{x}}^T \partial f(\mathbf{x}) - \bar{\eta}^T \partial \partial f(\mathbf{x}) \eta. \quad (A5)$$

946 These two terms are precisely the exponential representation  
947 of the Dirac  $\delta$  function of the gradient and determinant of the  
948 Hessian (without absolute value sign) that make up the basic  
949 Kac–Rice measure, so that we can write

$$\begin{aligned} &\int d\mathbf{x} \delta(\nabla H(\mathbf{x})) \det \text{Hess } H(\mathbf{x}) \\ &= \int d\mathbf{x} d\bar{\eta} d\eta \frac{d\hat{\mathbf{x}}}{(2\pi)^N} e^{i\hat{\mathbf{x}}^T \nabla H(\mathbf{x}) - \bar{\eta}^T \text{Hess } H(\mathbf{x}) \eta} \\ &= \int d\phi e^{\int d1 H(\phi(1))}, \end{aligned} \quad (A6)$$

950 where we have written the measures  $d1 = d\theta_1 d\bar{\theta}_1$  and  $d\phi =$   
951  $d\mathbf{x} d\bar{\eta} d\eta \frac{d\hat{\mathbf{x}}}{(2\pi)^N}$ . Besides some deep connections to the physics  
952 of BRST, this compact notation dramatically simplifies the  
953 analytical treatment of the problem. The energy of stationary  
954 points can also be fixed using this notation by writing

$$\int d\phi d\hat{\beta} e^{\hat{\beta} E + \int d1 (1 - \hat{\beta} \bar{\theta}_1 \theta_1) H(\phi(1))}, \quad (A7)$$

955 which a small calculation confirms results in the same expres-  
956 sion as (35).

957 The reason why this transformation is a simplification is  
958 because there are a large variety of superspace algebraic and  
959 integral operations with direct corollaries to their ordinary real  
960 counterparts. For instance, consider a super linear operator  
961  $M(1, 2)$ , which like the super vector  $\phi$  is made up of a linear  
962 combination of  $N \times N$  regular or Grassmann matrices indexed  
963 by every nonvanishing combination of the Grassmann indices  
964  $\bar{\theta}_1, \theta_1, \bar{\theta}_2, \theta_2$ . Such a supermatrix acts on supervectors by  
965 ordinary matrix multiplication and convolution in the Grass-  
966 mann indices, i.e.,

$$(M\phi)(1) = \int d2 M(1, 2)\phi(2). \quad (\text{A8})$$

967 The identity supermatrix is given by

$$\delta(1, 2) = (\bar{\theta}_1 - \bar{\theta}_2)(\theta_1 - \theta_2)I. \quad (\text{A9})$$

968 Integrals involving superfields contracted into such operators  
969 result in schematically familiar expressions, like that of the  
970 standard Gaussian:

$$\int d\phi e^{-\frac{1}{2} \int d1 d2 \phi(1)^T M(1, 2) \phi(2)} = (\text{sdet } M)^{-1/2}, \quad (\text{A10})$$

971 where the usual role of the determinant is replaced by the  
972 superdeterminant. The superdeterminant can be defined us-  
973 ing the ordinary determinant by writing a block version of  
974 the matrix  $M$ . If  $\mathbf{e}(1) = \{1, \bar{\theta}_1\theta_1\}$  is the basis vector of the  
975 even subspace of the superspace and  $\mathbf{f}(1) = \{\bar{\theta}_1, \theta_1\}$  is that  
976 of the odd subspace, dual bases  $\mathbf{e}^\dagger(1) = \{\bar{\theta}_1\theta_1, 1\}$  and  $\mathbf{f}^\dagger(1) =$   
977  $\{-\theta_1, \bar{\theta}_1\}$  can be defined by the requirement that

$$\int d1 e_i^\dagger(1) e_j(1) = \delta_{ij}, \quad \int d1 f_i^\dagger(1) f_j(1) = \delta_{ij}, \quad (\text{A11})$$

$$\int d1 e_i^\dagger(1) f_j(1) = 0, \quad \int d1 f_i^\dagger(1) e_j(1) = 0. \quad (\text{A12})$$

978 With such bases and dual bases defined, we can form a block  
979 representation of  $M$  in analogy with the matrix form of an  
980 operator in quantum mechanics by

$$\int d1 d2 \begin{bmatrix} \mathbf{e}^\dagger(1)M(1, 2)\mathbf{e}(2) & \mathbf{e}^\dagger(1)M(1, 2)\mathbf{f}(2) \\ \mathbf{f}^\dagger(1)M(1, 2)\mathbf{e}(2) & \mathbf{f}^\dagger(1)M(1, 2)\mathbf{f}(2) \end{bmatrix} \\ = \begin{bmatrix} A & B \\ C & D \end{bmatrix}, \quad (\text{A13})$$

981 where each of the blocks is a  $2N \times 2N$  real matrix. Then the  
982 superdeterminant of  $M$  is given by

$$\text{sdet } M = \det(A - BD^{-1}C) \det(D)^{-1}, \quad (\text{A14})$$

983 which is the same as the normal expression for the determi-  
984 nant of a block matrix save for the inverse of  $\det D$ . Likewise,  
985 the supertrace of  $M$  is given by

$$\text{sTr } M = \text{Tr } A - \text{Tr } D. \quad (\text{A15})$$

986 The same method can be used to calculate the superdetermi-  
987 nant and supertrace in arbitrary superspaces, where for  
988  $\mathbb{R}^{N|2D}$  each basis has  $2^{2D-1}$  elements. For instance, for  $\mathbb{R}^{N|4}$

we have

$$\mathbf{e}(1, 2) = \{1, \bar{\theta}_1\theta_1, \bar{\theta}_2\theta_2, \bar{\theta}_1\theta_2, \bar{\theta}_2\theta_1, \bar{\theta}_1\bar{\theta}_2, \theta_1\theta_2, \bar{\theta}_1\theta_1\bar{\theta}_2\theta_2\}, \\ \mathbf{f}(1, 2) = \{\bar{\theta}_1, \theta_1, \bar{\theta}_2, \theta_2, \bar{\theta}_1\theta_1\bar{\theta}_2, \bar{\theta}_2\theta_2\theta_1, \bar{\theta}_1\theta_1\theta_2, \bar{\theta}_2\theta_2\theta_1\}, \quad (\text{A16})$$

with the dual bases defined analogously to those above.

## APPENDIX B: BECCHI-ROUET-STORA-TYUTIN SYMMETRY

993 When the trace  $\mu$  is not fixed, there is an unusual symmetry  
994 in the dominant complexity of minima [30–32]. This arises  
995 from considering the Kac–Rice formula as a kind of gauge  
996 fixing procedure [57]. Around each stationary point consider  
997 making the coordinate transformation  $\mathbf{u} = \nabla H(\mathbf{x})$ . Then, in  
998 the absence of fixing the trace of the Hessian to  $\mu$ , the Kac–  
999 Rice measure becomes

$$\int d\nu(\mathbf{x}, \omega|E) = \int \sum_{\sigma} d\mathbf{u} \delta(\mathbf{u}) \delta(NE - H(\mathbf{x}_{\sigma})), \quad (\text{B1})$$

1000 where the sum is over stationary points  $\sigma$ . This integral has a  
1001 symmetry of its measure of the form  $\mathbf{u} \mapsto \mathbf{u} + \delta\mathbf{u}$ . Under the  
1002 nonlinear transformation that connects  $\mathbf{u}$  and  $\mathbf{x}$ , this implies  
1003 a symmetry of the measure in the Kac–Rice integral of  $\mathbf{x} \mapsto$   
1004  $\mathbf{x} + (\text{Hess } H)^{-1} \delta\mathbf{u}$ . This symmetry, while exact, is nonlinear  
1005 and difficult to work with.

1006 When the absolute value function has been dropped and  
1007 Grassmann vectors introduced to represent the determinant  
1008 of the Hessian, this symmetry can be simplified considerably.  
1009 Due to the expansion properties of Grassmann integrals, any  
1010 appearance of  $-\bar{\eta}\eta^T$  in the integrand resolves to  $(\text{Hess } H)^{-1}$ .  
1011 The symmetry of the measure can then be written

$$\mathbf{x} \mapsto \mathbf{x} - \bar{\eta}\eta^T \delta\mathbf{u} = \mathbf{x} + \bar{\eta}\delta\epsilon, \quad (\text{B2})$$

1012 where  $\delta\epsilon = -\eta^T \delta\mathbf{u}$  is a Grassmann number. This establishes  
1013 that  $\delta\mathbf{x} = \bar{\eta}\delta\epsilon$ , now linear. The rest of the transformation can  
1014 be built by requiring that the action is invariant after expansion  
1015 in  $\delta\epsilon$ . This gives

$$\delta\mathbf{x} = \bar{\eta}\delta\epsilon, \quad \delta\hat{\mathbf{x}} = -i\hat{\beta}\bar{\eta}\delta\epsilon, \quad \delta\eta = -i\hat{\mathbf{x}}\delta\epsilon, \quad \delta\bar{\eta} = 0, \quad (\text{B3})$$

so that the differential form of the symmetry is

$$\mathcal{D} = \bar{\eta} \cdot \frac{\partial}{\partial \mathbf{x}} - i\hat{\beta}\bar{\eta} \cdot \frac{\partial}{\partial \hat{\mathbf{x}}} - i\hat{\mathbf{x}} \cdot \frac{\partial}{\partial \eta}, \quad (\text{B4})$$

1017 The Ward identities associated with this symmetry give rise  
1018 to relationships among the order parameters. These identities  
1019 come from applying the differential symmetry to Grassmann-  
1020 valued order parameters and are

$$0 = \frac{1}{N} \mathcal{D} \langle \mathbf{x}_a \cdot \eta_b \rangle = \frac{1}{N} [ \langle \bar{\eta}_a \cdot \eta_b \rangle - i \langle \mathbf{x}_a \cdot \hat{\mathbf{x}}_b \rangle ] \\ = G_{ab} + R_{ab}, \quad (\text{B5})$$

$$0 = \frac{i}{N} \mathcal{D} \langle \hat{\mathbf{x}}_a \cdot \eta_b \rangle = \frac{1}{N} [ \langle \hat{\beta} \bar{\eta}_a \cdot \eta_b \rangle + \langle \hat{\mathbf{x}}_a \cdot \hat{\mathbf{x}}_b \rangle ] \\ = \hat{\beta} G_{ab} + D_{ab}. \quad (\text{B6})$$

1021 These identities establish  $G_{ab} = -R_{ab}$  and  $D_{ab} = \hat{\beta} R_{ab}$ , al-  
1022 lowing elimination of the matrices  $G$  and  $D$  in favor of  $R$ .  
1023 Fixing the trace to  $\mu$  explicitly breaks this symmetry, and the  
1024 simplification is lost.

**APPENDIX C: SPECTRAL DENSITY IN THE MULTISPHERICAL SPIN GLASS**

In this Appendix we derive an expression for the asymptotic spectral density of the Hessian in the two-sphere multispherical spin glass that we describe in Sec. IV B. We use a typical approach of employing replicas to compute the resolvent [58]. The resolvent for the Hessian of the multispherical model is given by an integral over  $\mathbf{y} = [\mathbf{y}^{(1)}, \mathbf{y}^{(2)}] \in \mathbb{R}^{2N}$  as

$$\begin{aligned} G(\lambda) &= \lim_{n \rightarrow 0} \int \|\mathbf{y}_1\|^2 \prod_{a=1}^n d\mathbf{y}_a \exp \left\{ -\frac{1}{2} \mathbf{y}_a^T (\text{Hess } H(\mathbf{x}, \omega) - \lambda I) \mathbf{y}_a \right\} \\ &= \lim_{n \rightarrow 0} \int (\|\mathbf{y}_1^{(1)}\|^2 + \|\mathbf{y}_1^{(2)}\|^2) \prod_{a=1}^n d\mathbf{y}_a \exp \left\{ -\frac{1}{2} \begin{bmatrix} \mathbf{y}_a^{(1)} \\ \mathbf{y}_a^{(2)} \end{bmatrix}^T \left( \begin{bmatrix} \partial_1 \partial_1 H_1(\mathbf{x}^{(1)}) + \omega_1 I & -\epsilon I \\ -\epsilon I & \partial_2 \partial_2 H_2(\mathbf{x}^{(2)}) + \omega_2 I \end{bmatrix} - \lambda I \right) \begin{bmatrix} \mathbf{y}_a^{(1)} \\ \mathbf{y}_a^{(2)} \end{bmatrix} \right\}. \end{aligned} \quad (\text{C1})$$

If  $Y_{ab}^{(ij)} = \frac{1}{N} \mathbf{y}_a^{(i)} \cdot \mathbf{y}_b^{(j)}$  is the matrix of overlaps of the vectors  $\mathbf{y}$ , then a short and standard calculation involving the average over  $H$  and the change of variables from  $\mathbf{y}$  to  $Y$  yields

$$\overline{G(\lambda)} = N \lim_{n \rightarrow 0} \int dY (Y_{11}^{(11)} + Y_{11}^{(22)}) e^{nNS(Y)}, \quad (\text{C2})$$

where the effective action  $\mathcal{S}$  is given by

$$\begin{aligned} \mathcal{S}(Y) &= \lim_{n \rightarrow 0} \frac{1}{n} \left\{ \frac{1}{4} \sum_{ab} [f_1''(1)(Y_{ab}^{(11)})^2 + f_2''(1)(Y_{ab}^{(22)})^2] + \frac{1}{2} \sum_a [2\epsilon Y_{aa}^{(12)} + (\lambda - \omega_1)Y_{aa}^{(11)} + (\lambda - \omega_2)Y_{aa}^{(22)}] \right. \\ &\quad \left. + \frac{1}{2} \log \det \begin{bmatrix} Y^{(11)} & Y^{(12)} \\ Y^{(12)} & Y^{(22)} \end{bmatrix} \right\}, \end{aligned} \quad (\text{C3})$$

Making the replica symmetric ansatz  $Y_{ab}^{(ij)} = y^{(ij)} \delta_{ab}$  for each of the matrices  $Y^{(ij)}$  yields

$$\mathcal{S}(y) = \frac{1}{4} [f_1''(1)(y^{(11)})^2 + f_2''(1)(y^{(22)})^2] + \epsilon y^{(12)} + \frac{1}{2} [(\lambda - \omega_1)y^{(11)} + (\lambda - \omega_2)y^{(22)}] + \frac{1}{2} \log(y^{(11)}y^{(22)} - y^{(12)}y^{(12)}), \quad (\text{C4})$$

while the average resolvent becomes

$$\overline{G(\lambda)} = N(y^{(11)} + y^{(22)}) \quad (\text{C5})$$

for  $y^{(11)}$  and  $y^{(22)}$  evaluated at a saddle point of  $\mathcal{S}$ . The spectral density at large  $N$  is then given by the discontinuity in its imaginary point on the real axis, or

$$\rho(\lambda) = \frac{1}{2\pi i N} (\overline{G(\lambda + i0^+)} - \overline{G(\lambda + i0^-)}). \quad (\text{C6})$$

**APPENDIX D: COMPLEXITY OF DOMINANT OPTIMA FOR SUMS OF SQUARED RANDOM FUNCTIONS**

Here we share an outline of the derivation of formulas for the complexity of dominant optima in sums of squared random functions of Sec. IV C. While in this paper we only treat problems with a replica symmetric structure, formulas for the effective action are generic to any RSB structure and provide a starting point for analyzing the challenging full RSB setting.

Using the  $\mathbb{R}^{N^2}$  superfields

$$\phi_a(1) = \mathbf{x}_a + \bar{\theta}_1 \eta_a + \bar{\eta}_a \theta_1 + \bar{\theta}_1 \theta_1 \hat{\mathbf{x}}_a, \quad (\text{D1})$$

the replicated count of stationary points can be written

$$\mathcal{N}(E, \mu)^n = \int d\hat{\beta} \prod_{a=1}^n d\phi_a \exp \left[ N\hat{\beta}E - \frac{1}{2} \int d1 \left( B(1) \sum_{k=1}^M V_k(\phi_a(1))^2 - (\mu + f'(0)) \|\phi_a(1)\|^2 \right) \right] \quad (\text{D2})$$

for  $B(1) = 1 - \hat{\beta} \bar{\theta}_1 \theta_1$ . The derivation of the complexity follows from here nearly identically to that in Appendix A.2 of Fyodorov and Tublin with superoperations replacing standard ones [44]. First we insert Dirac  $\delta$  functions to fix each of the  $M$  energies  $V_k(\phi_a(1))$  as

$$\delta(V_k(\phi_a(1)) - v_{ka}(1)) = \int d\hat{v}_{ka} \exp \left[ i \int d1 \hat{v}_{ka}(1) (V_k(\phi_a(1)) - v_{ka}(1)) \right]. \quad (\text{D3})$$

1045 The squared  $V_k$  appearing in the energy can now be replaced by the variables  $v_k$ , leaving the only remaining dependence on the  
 1046 disordered  $V$  in the contribution of (D3), which is linear. The average over the disorder can then be computed, which yields

$$\exp \left[ i \sum_{k=1}^M \sum_{a=1}^n \int d1 \hat{v}_{ka}(1) V_k(\phi_a(1)) \right] = \exp \left[ -\frac{1}{2} \sum_{k=1}^M \sum_{ab}^n \int d1 d2 \hat{v}_{ka}(1) f \left( \frac{\phi_a(1) \cdot \phi_b(2)}{N} \right) \hat{v}_{kb}(2) \right]. \quad (\text{D4})$$

1047 The result is factorized in the indices  $k$  and Gaussian in the superfields  $v$  and  $\hat{v}$  with kernel

$$\begin{bmatrix} B(1) \delta_{ab} \delta(1, 2) & i \delta_{ab} \delta(1, 2) \\ i \delta_{ab} \delta(1, 2) & f \left( \frac{\phi_a(1) \cdot \phi_b(2)}{N} \right) \end{bmatrix}. \quad (\text{D5})$$

1048 Making the  $M$  independent Gaussian integrals, we find

$$\begin{aligned} \mathcal{N}(E, \mu)^n &= \int d\hat{\beta} \left( \prod_{a=1}^n d\phi_a \right) \exp \left\{ nN \hat{\beta} E + \frac{\mu + f'(0)}{2} \sum_a^n \int d1 \|\phi_a\|^2 \right. \\ &\quad \left. - \frac{M}{2} \log \text{sdet} \left[ \delta_{ab} \delta(1, 2) + B(1) f \left( \frac{\phi_a(1) \cdot \phi_b(2)}{N} \right) \right] \right\}. \end{aligned} \quad (\text{D6})$$

1049 We make a change of variables from the fields  $\phi$  to matrices  $\mathbb{Q}_{ab}(1, 2) = \frac{1}{N} \phi_a(1) \cdot \phi_b(2)$ . This transformation results in a change  
 1050 of measure of the form

$$\prod_{a=1}^n d\phi_a = d\mathbb{Q} (\text{sdet } \mathbb{Q})^{\frac{N}{2}} = d\mathbb{Q} \exp \left[ \frac{N}{2} \log \text{sdet } \mathbb{Q} \right]. \quad (\text{D7})$$

1051 We therefore have

$$\mathcal{N}(E, \mu)^n = \int d\hat{\beta} d\mathbb{Q} \exp \left\{ nN \hat{\beta} E + N \frac{\mu + f'(0)}{2} \text{sTr } \mathbb{Q} + \frac{N}{2} \log \text{sdet } \mathbb{Q} - \frac{M}{2} \log \text{sdet} [\delta_{ab} \delta(1, 2) + B(1) f(\mathbb{Q}_{ab}(1, 2))] \right\}. \quad (\text{D8})$$

1052 We now need to blow up our supermatrices into our physical order parameters. We have from the definition of  $\phi$  and  $\mathbb{Q}$  that

$$\mathbb{Q}_{ab}(1, 2) = C_{ab} - G_{ab}(\bar{\theta}_1 \theta_2 + \bar{\theta}_2 \theta_1) - R_{ab}(\bar{\theta}_1 \theta_1 + \bar{\theta}_2 \theta_2) - D_{ab} \bar{\theta}_1 \theta_2 \bar{\theta}_2 \theta_2, \quad (\text{D9})$$

1053 where  $C, R, D$ , and  $G$  are the matrices defined in (48). Other possible combinations involving scalar products between fermionic  
 1054 and bosonic variables do not contribute at physical saddle points [34]. Inserting this expansion into the expression above and  
 1055 evaluating the superdeterminants and supertrace, we find

$$\mathcal{N}(E, \mu)^n = \int d\hat{\beta} dC dR dD dG e^{nS_{\text{KR}}(\hat{\beta}, C, R, D, G)}, \quad (\text{D10})$$

1056 where the effective action is given by

$$\begin{aligned} S_{\text{KR}}(\hat{\beta}, C, R, D, G) &= \hat{\beta} E + \lim_{n \rightarrow 0} \frac{1}{n} \left( -(\mu + f'(0)) \text{Tr}(G + R) + \frac{1}{2} \log \det[G^{-2}(CD + R^2)] + \alpha \log \det[I + G \odot f'(C)] \right. \\ &\quad \left. - \frac{\alpha}{2} \log \det[(f'(C) \odot D - \hat{\beta} I + (G^{\odot 2} - R^{\odot 2}) \odot f''(C)) f(C) + (I - R \odot f'(C))^2] \right), \end{aligned} \quad (\text{D11})$$

1057 where  $\odot$  gives the Hadamard or componentwise product between the matrices and  $A^{\odot n}$  gives the Hadamard power of  $A$ , while  
 1058 other products and powers are matrix products and powers.

1059 In the case where  $\mu$  is not specified, we can make use of the BRST symmetry of Appendix B whose Ward identities give  
 1060  $D = \hat{\beta} R$  and  $G = -R$ . Using these relations, the effective action becomes particularly simple:

$$S_{\text{KR}}(\hat{\beta}, C, R) = \hat{\beta} E + \frac{1}{2} \lim_{n \rightarrow 0} \frac{1}{n} (\log \det(I + \hat{\beta} C R^{-1}) - \alpha \log \det[I - \hat{\beta} f(C)(I - R \odot f'(C))^{-1}]). \quad (\text{D12})$$

1061 This effective action is general for arbitrary matrices  $C$  and  $R$ , and therefore arbitrary RSB order. When using a replica symmetric  
 1062 ansatz of  $C_{ab} = \delta_{ab} + c_0(1 - \delta_{ab})$  and  $R_{ab} = r\delta_{ab} + r_0(1 - \delta_{ab})$ , the resulting function of  $\hat{\beta}, c_0, r$ , and  $r_0$  is

$$\begin{aligned} S_{\text{KR}}(\hat{\beta}, c_0, r, r_0) &= \hat{\beta} E + \frac{1}{2} \left[ \log \left( 1 + \frac{\hat{\beta}(1 - c_0)}{r - r_0} \right) + \frac{\hat{\beta} c_0 + r_0}{\hat{\beta}(1 - c_0) + r - r_0} - \frac{r_0}{r - r_0} \right] - \frac{\alpha}{2} \left[ \log \left( 1 - \frac{\hat{\beta}(f(1) - f(c_0))}{1 - r f'(1) + r_0 f'(c_0)} \right) \right. \\ &\quad \left. - \frac{\hat{\beta} f(c_0) + r_0 f'(c_0)}{1 - \hat{\beta}(f(1) - f(c_0)) - r f'(1) + r_0 f'(c_0)} + \frac{r_0 f'(c_0)}{1 - r f'(1) + r_0 f'(c_0)} \right]. \end{aligned} \quad (\text{D13})$$

1063 When  $f(0) = 0$  as in the cases directly studied in this work, this further simplifies as  $c_0 = r_0 = 0$ . The effective action is then

$$\mathcal{S}_{\text{KR}}(\hat{\beta}, r) = \hat{\beta}E + \frac{1}{2} \log \left( 1 + \frac{\hat{\beta}}{r} \right) - \frac{\alpha}{2} \log \left( 1 - \frac{\hat{\beta}f(1)}{1 - rf'(1)} \right). \quad (\text{D14})$$

1064 Extremizing this expression with respect to the order parameters  $\hat{\beta}$  and  $r$  produces the red line of dominant minima shown in  
1065 Fig. 3.

- 
- [1] V. Ros and Y. V. Fyodorov, The high-dimensional landscape paradigm: Spin-glasses, and beyond, in *Spin Glass Theory and Far Beyond* (World Scientific, 2023), pp. 95–114.
- [2] G. Biroli and J. P. Garrahan, Perspective: The glass transition, *J. Chem. Phys.* **138**, 12A301 (2013).
- [3] F. Krzakala and J. Kurchan, Landscape analysis of constraint satisfaction problems, *Phys. Rev. E* **76**, 021122 (2007).
- [4] G. Folena, S. Franz, and F. Ricci-Tersenghi, Rethinking mean-field glassy dynamics and its relation with the energy landscape: The surprising case of the spherical mixed  $p$ -spin model, *Phys. Rev. X* **10**, 031045 (2020).
- [5] G. Folena and F. Zamponi, On weak ergodicity breaking in mean-field spin glasses, *SciPost Phys.* **15**, 109 (2023).
- [6] A. El Alaoui and A. Montanari, Algorithmic thresholds in mean field spin glasses, [arXiv:2009.11481](https://arxiv.org/abs/2009.11481).
- [7] J. Kent-Dobias and J. Kurchan, How to count in hierarchical landscapes: A full solution to mean-field complexity, *Phys. Rev. E* **107**, 064111 (2023).
- [8] M. Müller and M. Wyart, Marginal stability in structural, spin, and electron glasses, *Annu. Rev. Condens. Matter Phys.* **6**, 177 (2015).
- [9] P. W. Anderson, Lectures on amorphous systems, in *III-Condensed Matter* (North-Holland Publishing Company, 1984), pp. 159–261.
- [10] H. J. Sommers and W. Dupont, Distribution of frozen fields in the mean-field theory of spin glasses, *J. Phys. C* **17**, 5785 (1984).
- [11] G. Parisi, On the statistical properties of the large time zero temperature dynamics of the SK model, [arXiv:cond-mat/9501045](https://arxiv.org/abs/cond-mat/9501045).
- [12] H. Horner, Time dependent local field distribution and metastable states in the SK-spin-glass, *Eur. Phys. J. B* **60**, 413 (2007).
- [13] S. Pankov, Low-temperature solution of the Sherrington-Kirkpatrick model, *Phys. Rev. Lett.* **96**, 197204 (2006).
- [14] V. Erba, F. Behrens, F. Krzakala, and L. Zdeborová, Quenches in the Sherrington–Kirkpatrick model, *J. Stat. Mech.: Theory Exp.* (2024) 083302.
- [15] A. L. Efros and B. I. Shklovskii, Coulomb interaction in disordered systems with localized electronic states, in *Electron–Electron Interactions in Disordered Systems*, Modern Problems in Condensed Matter Sciences, Vol. 10 (Elsevier, 1985), pp. 409–482.
- [16] B. I. Shklovskii, Half century of Efros-Shklovskii Coulomb gap. romance with Coulomb interaction and disorder, *Low Temp. Phys.* **50**, 1226 (2024).
- [17] G. Folena and P. Urbani, Marginal stability of soft anharmonic mean field spin glasses, *J. Stat. Mech.: Theory Exp.* (2022) 053301.
- [18] R. Monasson, Structural glass transition and the entropy of the metastable states, *Phys. Rev. Lett.* **75**, 2847 (1995).
- [19] Y. V. Fyodorov, Complexity of random energy landscapes, glass transition, and absolute value of the spectral determinant of random matrices, *Phys. Rev. Lett.* **92**, 240601 (2004).
- [20] A. J. Bray and D. S. Dean, Statistics of critical points of Gaussian fields on large-dimensional spaces, *Phys. Rev. Lett.* **98**, 150201 (2007).
- [21] J. Kent-Dobias, Algorithm-independent bounds on complex optimization through the statistics of marginal optima, [arXiv:2407.02092](https://arxiv.org/abs/2407.02092) [cond-mat.dis-nn] ().
- [22] H. Ikeda, Bose–Einstein-like condensation of deformed random matrix: a replica approach, *J. Stat. Mech.: Theory Exp.* (2023) 023302.
- [23] J. Kent-Dobias, Arrangement of nearby minima and saddles in the mixed spherical energy landscapes, *SciPost Phys.* **16**, 001 (2024).
- [24] Y. V. Fyodorov and P. Le Doussal, Topology trivialization and large deviations for the minimum in the simplest random optimization, *J. Stat. Phys.* **154**, 466 (2014).
- [25] Y. V. Fyodorov and P. Le Doussal, Hessian spectrum at the global minimum of high-dimensional random landscapes, *J. Phys. A: Math. Theor.* **51**, 474002 (2018).
- [26] D. S. Dean and S. N. Majumdar, Large deviations of extreme eigenvalues of random matrices, *Phys. Rev. Lett.* **97**, 160201 (2006).
- [27] J. Kent-Dobias, On the topology of solutions to random continuous constraint satisfaction problems, [arXiv:2409.12781](https://arxiv.org/abs/2409.12781) [cond-mat.dis-nn] ().
- [28] M. Kac, On the average number of real roots of a random algebraic equation, *Bull. Am. Math. Soc.* **49**, 314 (1943).
- [29] S. O. Rice, The distribution of the maxima of a random curve, *Am. J. Math.* **61**, 409 (1939).
- [30] A. Annibale, A. Cavagna, I. Giardina, and G. Parisi, Supersymmetric complexity in the Sherrington–Kirkpatrick model, *Phys. Rev. E* **68**, 061103 (2003).
- [31] A. Annibale, A. Cavagna, I. Giardina, G. Parisi, and E. Trevisani, The role of the Becchi–Rouet–Stora–Tyutin supersymmetry in the calculation of the complexity for the Sherrington–Kirkpatrick model, *J. Phys. A: Math. Gen.* **36**, 10937 (2003).
- [32] A. Annibale, G. Gualdi, and A. Cavagna, Coexistence of supersymmetric and supersymmetry-breaking states in spherical spin-glasses, *J. Phys. A: Math. Gen.* **37**, 11311 (2004).
- [33] A. Crisanti, H. Horner, and H.-J. Sommers, The spherical  $p$ -spin interaction spin-glass model, *Z. Phys. B: Condens. Matter* **92**, 257 (1993).
- [34] J. Kurchan, Supersymmetry in spin glass dynamics, *J. Phys. I* **2**, 1333 (1992).
- [35] E. Subag, TAP approach for multi-species spherical spin glasses I: General theory, [arXiv:2111.07132](https://arxiv.org/abs/2111.07132) [math.PR].

- [36] E. Subag, TAP approach for multispecies spherical spin glasses II: The free energy of the pure models, *Ann. Probab.* **51**, 1004 (2023).
- [37] E. Bates and Y. Sohn, Crisanti–Sommers formula and simultaneous symmetry breaking in multi-species spherical spin glasses, *Commun. Math. Phys.* **394**, 1101 (2022).
- [38] E. Bates and Y. Sohn, Free energy in multi-species mixed  $p$ -spin spherical models, *Electron. J. Probab.* **27**, 1 (2022).
- [39] B. Huang and M. Sellke, Strong topological trivialization of multi-species spherical spin glasses, [arXiv:2308.09677](https://arxiv.org/abs/2308.09677) [math.PR] ().
- [40] B. Huang and M. Sellke, Algorithmic threshold for multi-species spherical spin glasses, [arXiv:2303.12172](https://arxiv.org/abs/2303.12172) [math.PR] ().
- [41] B. Huang and M. Sellke, Optimization algorithms for multi-species spherical spin glasses, *J. Stat. Phys.* **191**, 29 (2024).
- [42] Y. V. Fyodorov, A spin glass model for reconstructing nonlinearly encrypted signals corrupted by noise, *J. Stat. Phys.* **175**, 789 (2019).
- [43] Y. V. Fyodorov and R. Tublin, Counting stationary points of the loss function in the simplest constrained least-square optimization, *Acta Phys. Pol. B* **51**, 1663 (2020).
- [44] Y. V. Fyodorov and R. Tublin, Optimization landscape in the simplest constrained random least-square problem, *J. Phys. A: Math. Theor.* **55**, 244008 (2022).
- [45] P. Vivo, Random linear systems with quadratic constraints: from random matrix theory to replicas and back, [arXiv:2401.03209](https://arxiv.org/abs/2401.03209) [cond-mat.stat-mech].
- [46] R. Tublin, A few results in random matrix theory and random optimization, Ph.D. thesis, King's College London (2022).
- [47] P. Urbani, A continuous constraint satisfaction problem for the rigidity transition in confluent tissues, *J. Phys. A: Math. Theor.* **56**, 115003 (2023).
- [48] P. J. Kamali and P. Urbani, Dynamical mean field theory for models of confluent tissues and beyond, *SciPost Phys.* **15**, 219 (2023).
- [49] P. J. Kamali and P. Urbani, Stochastic gradient descent outperforms gradient descent in recovering a high-dimensional signal in a glassy energy landscape, [arXiv:2309.04788](https://arxiv.org/abs/2309.04788) [cs.LG].
- [50] A. Montanari and E. Subag, Solving overparametrized systems of random equations: I. model and algorithms for approximate solutions, [arXiv:2306.13326](https://arxiv.org/abs/2306.13326) [math.PR] ().
- [51] A. Montanari and E. Subag, On Smale's 17th problem over the reals, [arXiv:2405.01735](https://arxiv.org/abs/2405.01735) [cs.DS] ().
- [52] P. Urbani, Statistical physics of complex systems: glasses, spin glasses, continuous constraint satisfaction problems, high-dimensional inference and neural networks, [arXiv:2405.06384](https://arxiv.org/abs/2405.06384) [cond-mat.dis-nn].
- [53] M. Müller, L. Leuzzi, and A. Crisanti, Marginal states in mean-field glasses, *Phys. Rev. B* **74**, 134431 (2006).
- [54] A. El Alaoui, A. Montanari, and M. Sellke, Sampling from the Sherrington-Kirkpatrick Gibbs measure via algorithmic stochastic localization, in *2022 IEEE 63rd Annual Symposium on Foundations of Computer Science (FOCS)* (IEEE, Denver, 2022), pp. 323–334.
- [55] A. Montanari, Optimization of the Sherrington–Kirkpatrick Hamiltonian, *SIAM J. Comput.* **FOCS19** (2021).
- [56] B. S. DeWitt, *Supermanifolds*, 2nd ed., Cambridge monographs on mathematical physics (Cambridge University Press, Cambridge, New York, 1992).
- [57] J. Zinn-Justin, *Quantum Field Theory and Critical Phenomena* (Clarendon Press, Oxford University Press, Oxford, New York, 2002).
- [58] G. Livan, M. Novaes, and P. Vivo, *Introduction to Random Matrices*, SpringerBriefs in Mathematical Physics, Vol. 26 (Springer International Publishing, 2018).